Elsevier Editorial System(tm) for Quaternary Science Reviews
Manuscript Draft

Manuscript Number: JQSR-D-13-00085R1

Title: Deglaciation of the central Barents Sea

Article Type: Special Issue: APEX II

Keywords: Quaternary; Deglaciation; Barents Sea; Seabed geomorphology; Ice stream; Ice shelf; Grounding zone; MSGL; Crevasse-squeeze ridges; Retreat moraine; Corrugation ridge; ATB; GZW.

Corresponding Author: Dr. Lilja Rún Bjarnadóttir, Ph.D.

Corresponding Author's Institution: Geological Survey of Norway (NGU)

First Author: Lilja Rún Bjarnadóttir, Ph.D.

Order of Authors: Lilja Rún Bjarnadóttir, Ph.D.; Monica C Winsborrow, PhD; Karin Andreassen, PhD

Abstract: The marine-based Barents Sea Ice Sheet covered the polar continental shelf north of Norway and western Russia during the Last Glacial Maximum. Initial ice sheet retreat along the western margin is well established, while the retreat pattern in the interior parts of the ice sheet remains poorly known. Here we present new geological data from the central Barents Sea, including the formerly disputed zone. The results are based on analysis of several marine geophysical datasets, including geomorphological mapping of multibeam swath bathymetry data and analysis of seismic and acoustic stratigraphy. The new results provide insights into the configuration and dynamics of the ice sheet during its retreat across the central Barents Sea. In particular they show clear changes in the location of the main ice divides and domes, with ice flow becoming gradually more topographically controlled as deglaciation progressed. Major troughs were characterised by episodic retreat and reoccurring cycles of fast and slow ice flow, sometimes leading to stagnation and ice shelf formation. Meanwhile, adjacent bank areas were covered by comparatively slowly retreating ice, although evidence of streaming ice is also seen locally.

Highlights:

- Present new geophysical data from the Russian and Norwegian central Barents Sea.
- New reconstructions of ice dynamics during deglaciation in central Barents Sea.
- Bjørnøyrenna Ice Stream underwent repeated cycles of stagnancy and fast flow.
- Ice shelves may repeatedly have formed in Bjørnøyrenna.
- Parallels to observations and modelling of Antarctic ice stream velocity cycles.

Deglaciation of the central Barents Sea

Lilja R. Bjarnadóttir[a, 1,*], Monica C. M. Winsborrow[b, 2], Karin Andreassen[a, c]

[a] Department of Geology, University of Tromsø, Dramsveien 201, N-9037, Norway
[b] Geological Survey of Norway (NGU), P.O. box 6315 Sluppen, N-7491 Trondheim, Norway
[c] Centre of Excellence for Arctic Gas Hydrate, Environment and Climate (CAGE), University of Tromsø, N-9037 Tromsø, Norway
[1]Now at Geological Survey of Norway (NGU), P.O. box 6315 Sluppen, N-7491 Trondheim, Norway
[2]Now at Statoil ASA, Mølnholtet 42, Harstad, Norway

*Corresponding author: E-mail: lilja.bjarnadottir@ngu.no, Tel: +47 73904288, Fax: +47 73921620
[b, 2] mowin@statoil.com; [a, c] karin.andreassen@uit.no

Abstract

The marine-based Barents Sea Ice Sheet covered the polar continental shelf north of Norway and western Russia during the Last Glacial Maximum. Initial ice sheet retreat along the western margin is well established, while the retreat pattern in the interior parts of the ice sheet remains poorly known. Here we present new geological data from the central Barents Sea, including the formerly disputed zone. The results are based on analysis of several marine geophysical datasets, including geomorphological mapping of multibeam swath bathymetry data and analysis of seismic and acoustic stratigraphy. The new results provide insights into the configuration and dynamics of the ice sheet during its retreat across the central Barents Sea. In particular they show clear changes in the location of the main ice divides and domes, with ice flow becoming gradually more topographically controlled as deglaciation progressed. Major troughs were characterised by episodic retreat and reoccurring cycles of fast and slow ice flow, sometimes leading to stagnation and ice shelf formation. Meanwhile, adjacent bank areas were covered by comparatively slowly retreating ice, although evidence of streaming ice is also seen locally.

Keywords

Quaternary, Deglaciation, Barents Sea, Seabed geomorphology, Ice stream, Ice shelf, Grounding zone, MSGL, Crevasse-squeeze ridges, Retreat moraine, Corrugation ridge, ATB, GZW

1 Introduction

Glacial geomorphology is a useful tool for reconstructing the configuration, dynamics, ice flow direction, subglacial thermal regime and retreat dynamics of former ice sheets (e.g. Ó Cofaigh et al., 2002; Ottesen et al., 2005). This paper describes hitherto unmapped glacial landforms on the seafloor of the central Barents Sea, and uses these, in combination with previously published accounts, to make a new reconstruction of the pattern and dynamics of deglaciation in the central Barents Sea. We expect this paper to be of interest to those working with the glacial history of the Barents Sea and neighbouring areas, as well as those working on modern and former ice stream environments, ice sheet dynamics and stability.

1.1 Regional setting

The Barents Sea (Fig.1) is an epicontinental sea characterised by several shallow bank areas (100-200 m bsl) and deeper troughs (200-500 m bsl), which have been subject to repeated glaciations during the late Cenozoic (Elverhøi and Solheim, 1983; Vorren et al., 1988). Early reconstructions of the Barents Sea Ice Sheet were based on relatively limited marine geophysical datasets (e.g. Elverhøi and Solheim, 1983; Kristoffersen et al., 1984; Solheim and Kristoffersen, 1984; Solheim et al., 1990; Svendsen et al., 2004), whilst early modelling attempts were based mainly on the elevations and age of raised shorelines on islands fringing the Barents Sea (Andersen 1981; Forman et al., 1995; Lambeck, 1996; Elverhøi et al. 1993). These lacked information from the central part of the palaeo-ice sheet and were not able to resolve palaeo-glacidynamics. Later reconstructions have, to a larger degree, incorporated effects of glacial dynamics, showing the location of major ice streams and domes (Landvik et al., 1998; Ottesen et al., 2005; Winsborrow et al., 2010), and deglaciation stages along the western margin of the Barents Sea are becoming increasingly well constrained (Landvik et al., 1998; Mangerud et al. 1998; Winsborrow et al., 2010; Rüther et al., 2011; Bjarnadóttir et al., 2013; Ingólfsson and Landvik, 2013). Favourable sea ice conditions over the past few years have allowed data collection east of Svalbard and new, more detailed reconstructions have emerged (Dowdeswell et al., 2010; Hogan et al., 2010a; Hogan et al., 2010b; Rüther, 2012; Andreassen et al., This volume). The central Barents Sea, however, has remained largely unsurveyed due to a long-standing dispute between Norway and Russia regarding the location of territorial boundaries (Fig. 1). The resolution of this in 2011 means that data collection in this area is now possible, and this paper presents some of the first datasets collected in the formerly disputed area.

2 Datasets and methods

Landforms were mapped in Esri ArcMap v.10.0 based on several different marine geophysical datasets. The fisheries database Olex (www.olex.no, 2010), and the International Bathymetric Chart of the Arctic Ocean (IBCAO; version 3.0) have the broadest coverage but relatively low resolution . Olex is a compilation of seafloor echo-soundings and covers the majority of the western Barents Sea. The Olex seafloor image has a vertical resolution of 0.1-1 m (depth-dependent), a lateral resolution of 5 m up to a few tens of metres and positional accuracy of <10 m (http://www.olex.no; Bradwell et al., 2008). IBCAO v.3 has a cell size of 500 m and consists of several different bathymetric datasets of varying resolution merged together (Jakobsson et al., 2012).

Higher resolution multibeam swath bathymetry data, acquired during several cruises using the University of Tromsø vessel R/V Helmer Hanssen (formerly R/V Jan Mayen) in the summers of 2008, 2010, 2011 and 2012, and the 18th Training Through Research (TTR-18) cruise using R/V Akademik Strakhov in 2011, are also used. The multibeam system on R/V Helmer Hanssen consists of a Kongsberg Simrad EM-300 multibeam (135 beams) echo sounder operating at 30 kHz, with 63° by 63° beam configuration and automatic continuous pinging. Sound speeds were calibrated by CTD profiles acquired with a Seabird 911. The data were processed in Kongsberg Neptune and gridded to 10x10 m. The multibeam system on R/V Akademik Strakhov is a Reson Seabat 8111/7111 multibeam swath echo sounder (101 beams) operating at 100 kHz, with 150° swath, and swath widths of ~800-1000 m at depths of 150-450 m bsl. The data were processed and gridded to 10x10 m in Reson PDS2000.

Subsurface data collected in areas 1-4 (Figs. 1-7) on R/V Helmer Hanssen include chirp data and single-channel seismic data. The chirp system is a hull-mounted, Edgetech HM-3300 system, with a 16-element transducer, using a signal length of 40 ms and sweeping 1.5-9 kHz. Maximum observed penetration into sediments was <40 ms. The single-channel seismic system included a 15/15 cubic inch mini GI-airgun (shot rate 3 sec), a 6 m long 20-element streamer, a BOGE Compair Reavell compressor (pressure regulated to 160 Bar). Data of frequencies 0-800 Hz was recorded using a windows-based Delph recorder and stored on hard drives in Elics format. The maximum observed penetration was ~850 ms. Subsurface data acquired during the TTR-18 cruise included sparker data in area 5 (Figs. 1, 8). The sparker data was acquired with a SONIC-4M system which consisted of a ~4 kJ high voltage power unit, a 6 channel streamer (5 m between channels), a 5 electrodes sparker with a dominant frequency of ~130 Hz, an analogue block (amplifier, 50 Hz low-cut filter, 2500 Hz high-cut filter) and A/D L-Card E440 (14 bit). The data were processed using RadEx Pro burst noise removal and band-pass filtered in Kingdom Suite. Maximum observed penetration was ~700 ms.

The distribution of glacial landforms and sediment packages were mapped based on the acoustic datasets. Relevant radiocarbon dates from previously published studies have been recalibrated in this study using Calib 6.0.1 (Stuiver and Reimer, 1993) with the IntCal09 and Marine09 curves (Reimer et al., 2009), using a ΔR value of 71±21 (Mangerud et al., 2006) and are given with 2σ range.

3 Results and discussion

Geomorphological mapping was carried out with the aim of reconstructing former ice sheet retreat patterns and dynamics and as such there was a focus on those features indicative of marginal positions (e.g. recessional moraines), and palaeo ice-flow directions (e.g. mega-scale glacial lineations (MSGLs)). The thickness and acoustic character of seafloor sediments were also investigated to identify grounding zone deposits and thereby former ice margin positions.

The large study area (encompassing much of the central Barents Sea) is divided into five areas (Fig. 1; areas 1-5), and for each a geomorphological map was produced showing landforms mapped based on new data, as well as features from previously published accounts (Figs. 2-6,8). These maps also include acoustic character, based on a combination of new chirp data and seismic data, along with results from other publications.

In the following section each of the five areas are taken in turn, and the geomorphic features identified are first described and interpreted, followed by a discussion of their formation and the information that they provide about past ice sheet configuration.

3.1 Area 1

Area 1 covers the middle and upper reaches of Bjørnøyrenna (Figs. 1, 2a, 3a). The trough is 120-460 m deep in this area and the bedrock consists of Mesozoic sedimentary rocks (Sigmond, 2002). Based on investigation of the Bjørnøyrenna Trough Mouth Fan and seafloor geomorphology of the trough, several papers have concluded that Bjørnøyrenna was occupied by a large ice stream during the last glaciation, which drained the interior of the Barents Sea Ice Sheet (e.g. Vorren and Laberg, 1996; Ottesen et al., 2005; Andreassen et al., 2008; Winsborrow et al., 2010; Rüther et al., 2011).

3.1.1 Slope breaks, ridges and grounding zone wedges

Based on analysis of the IBCAO v.3 dataset and the Olex seafloor image, major trough-transverse ridges (10-20 m high and 4-8 km wide) and major breaks in seafloor slope in Bjørnøyrenna were mapped (Fig. 2a). These features are broadly parallel to each other, often spanning the whole width of the trough and terminating on the trough flanks. Available chirp data across the features reveal that in several cases, acoustically transparent sediment bodies (ATBs) occur in association with these mapped ridges/slope breaks (Fig. 3a). The ATBs often occur immediately downstream of mapped ridges/slope breaks and extend downstream for up to ~40 km, sometimes across more than one ridge/slope break (Fig. 3a, f). In some instances, the mapped ridge features appear to be bedrock protrusions (Fig. 3b, c, f). The ATBs have slightly lobate fronts and a smooth, slightly convex surface (Fig. 2g). Their downstream fronts can be either steeply convex or smooth out the seafloor surface by filling in underlying depressions. They are typically around 10-20 ms thick and form positive topographic features of varying height (Fig. 3). Sometimes the ATBs rise well above the surrounding seafloor (e.g. Fig. 3b), however the greatest thicknesses are seen where they fill in underlying depressions (Fig. 3d, e, f). Solheim et al. (1990) described the ATB sediments (just north of 76 °N in Fig. 3) as normally consolidated and consisting mainly of mud and sand. This fits well with the observed acoustic transparency and indicates that the ATBs are made up of homogenous and probably rather fine-grained sediments.

The distribution and characteristics of ATBs correspond closely to published accounts of sediment accumulations from this area (Fig. 3a; Elverhøi and Solheim, 1983; Kristoffersen et al., 1984; Solheim and Kristoffersen, 1984; Solheim et al., 1990). In these accounts they are interpreted to form through rapid deposition from turbid meltwater plumes emerging along ice margins. Other grounding line processes such as sediment rain-out from the ice margin and icebergs, direct pushing of sediment by the ice margin, squeeze-out of deforming sediments from beneath the grounding line and/or redeposition by proglacial slumping, make a smaller contribution (Elverhøi and Solheim, 1983; Solheim and Kristoffersen, 1984; Kristoffersen et al., 1984; Solheim and Pfirman, 1985; Solheim et al., 1990; Bjarnadóttir et al., 2013). An alternative explanation for the formation of ATBs was suggested by Epshtein et al. (2011b), who attributed them to deposition in zones of enhanced basal melting beneath the inner parts of ice sheets, where their normal consolidation is a result of the amount of subglacial meltwater exceeding the drainage capacity of the substrate. However, the distribution of landforms (described in chapters 3.1.2-3.1.5) is not compatible with the ideas of Epshtein et al. (2011b), and rather suggests that the ATBs are deposited in ice stream grounding zones.

In plan form the ATBs resemble grounding zone wedges (GZWs; e.g. Powell and Alley, 1997), and we have chosen to use the term grounding zone wedge (GZW; non-generic sense) for the ATBs. However, we note several key differences between documented GZWs and the ATBs described herein. Firstly, in cross section the ATBs are not necessarily wedge-shaped and are thinner (Dowdeswell and Fugelli, 2012). Secondly, ATBs lack dipping and/or hummocky internal reflections which are indicative of down-slope movement and pushing of sediments respectively. We interpret these differences to indicate that the main depositional processes during formation differed in either type and/or magnitude, with ATBs deposited primarily from sediment-laden meltwater plumes emerging along the ice sheet grounding line, but also influenced by the other grounding line processes such as sediment rain-out/squeeze-out and/or redeposition by pushing/low density debris flows. This style of margin-wide drainage and deposition has previously been described in settings of distributed drainage systems and leaky margins (cf. Powell and Alley, 1997), which we suggest may apply for the GZWs described here. A further discussion regarding this is given in chapter 4.3.

Solheim and Pfirman (1985) suggested that the crest of the ATB marks the position of the ice margin, thereby representing the boundary between the subglacial and proglacial environment. The ATBs mapped in this study do not always have well defined crests, making it hard to determine exact palaeo-ice margin positions. Furthermore, Andreassen et al. (This volume) suggested that the similar acoustic character of the inferred subglacial and proglacial parts of an ATB in upper Bjørnøyrenna (ice margin position 9 in Figs. 2a, 3a), may indicate a gradual transition from a subglacial to a proglacial environment. This commonly applies for GZWs which form where ice streams halt, sometimes repeatedly, during overall retreat. The upper boundaries of the Bjørnøyrenna ATBs may represent both the youngest palaeo-ice margin positions and/or the upper extent of near-floatation ice, and likewise downstream thickness maxima likely represent former grounding zones (Fig. 3a). In the cases where the ATBs consist of more than one main thickness maxima separated by areas of thinner acoustically transparent sediments (e.g. Fig. 3f), we suggest they represent several stillstand positions within the same retreat event. Due to low chirp penetration of the remaining trough-transverse ridge features, we were not able to confirm whether they are sedimentary or bedrock features. Nonetheless, we consider it likely that they too represent intermittent positions of ice margin stillstand during overall retreat. During the retreat of the Bjørnøyrenna Ice Stream across these features, protruding bedrock ridges and major slope breaks may have served as pinning points for the ice stream, allowing it to linger for a prolonged period at these points and preventing very rapid retreat.

Although different processes have been suggested for the formation of GZWs, they are commonly associated with warm-based and dynamic ice, where high basal water pressure facilitate fast ice flow (Dowdeswell and Fugelli, 2012). We suggest that this is the case also for the GZWs described in this paper. Furthermore, conclusions have been drawn about the style of ice retreat based on the distribution of GZWs within a trough. A pattern such as the one described for Bjørnøyrenna, would for example indicate that ice stream retreat occurred in an episodic manner (Ó Cofaigh et al. 2008; Dowdeswell et al. 2008). We thus conclude that the Bjørnøyrenna ice stream retreated in an episodic manner, experiencing fast retreat punctuated with still-stands and even readvances, with GZWs deposited in the ice stream grounding zone.

3.1.2 Small retreat ridges and ice-fingerprints

In the northwest corner of area 1 (Fig. 1), a network of slightly sinuous, yet aligned ridges oriented N-S and NNE-SSW, has been mapped (Fig. 2b). They are 2-12 m high, 90-400 m wide and more than 8 km long. We interpret them as recessional ridges, probably formed by ice margin push during minor winter readvances (e.g. Boulton 1986) and representing slow and steady ice retreat (Ottesen and Dowdeswell, 2006, 2009). There is no indication of fast ice flow in relation to these ridges and basal water pressure is thus inferred to have been low during their formation. The ridges run across the floor of an elongated depression interpreted as a tunnel valley by Bjarnadóttir et al. (2012), within which the ridges maintain their general direction but have a different appearance. Here they are characterised by chains of crescentic or convex-downstream ridges. Each crescentic ridge fronts an upstream depression, measures 150-400 m between the upstream ends and extend in a downslope direction by up to ~500 m at a near-normal angle to the linear trend (Fig. 2b). We suggest that these features are formed by ploughing or pushing of sediment by advancing fingers of grounded ice at the ice front and will hereafter refer to them as ice-fingerprints. Such ice-fingers can form if the margin experiences transverse extension (Geirsdóttir et al., 2008). We suggest that the transverse extension in this case can be attributed to a slightly larger advance of the ice within the deeper tunnel valley than on the flanking bank areas. The fact that ice-fingerprints only deviate slightly from the retreat ridges seems to contradict formation by iceberg ploughing. However, we cannot rule out the possibility that some of the ice-fingerprints are formed through ploughing by calved icebergs just off the ice margin.

3.1.3 Stagnation features

Large parts of the seafloor in area 1 are covered by trough-transverse/semi-transverse linear ridge segments (Fig. 2c) or polygonal and/or rhombohedral networks of sediment ridges (Fig. 2f) The ridges are <4 m high, 100 m wide and <1 km long (may extend outside the reach of the data). Where they form polygonal/rhombohedral networks the spacing between ridges is 70-180 m. A degree of longitudinal banding is observed on some of the transverse linear ridges (Fig. 2c). The observed longitudinal banding is ~1 km wide. The ridges are little disturbed by iceberg ploughmarks. Solheim et al. (1990) observed ridge features similar to these on side-scan sonar records from the area and interpreted them to be De Geer moraines. However, given the irregular and branching nature of the ridges, we disagree with this interpretation and instead consider it more likely that they are crevasse-squeeze ridges and relate to stagnation of the Bjørnøyrenna Ice Stream. Crevasse-squeeze ridges form by the displacement of subglacial sediments into basal crevasses (Sharp, 1985; Van der Veen, 1998), as ice flow regime switches from fast extensional ice-flow to stagnation, such as during the termination of surges (Solheim and Pfirman, 1985; Ottesen and Dowdeswell, 2006).

Stagnation features in sub-aerial locations are subject to intense meltwater erosion, down-wasting and weathering, meaning that although ice streams can stagnate repeatedly (e.g. Retzlaff and Bentley, 1993; Hulbe and Fahnestock, 2007), examples of landforms documenting these changes are rare in the palaeo-record. One example are features described by Patterson (1997), in association with known marginal positions of a major ice stream of the Laurentide Ice Sheet (Des Moines lobe), and attributed to repeated stagnation of the ice stream. The preservation potential of submarine stagnation features is higher and several nice examples have been described in front of surging tide-water glaciers in Svalbard (Ottesen and Dowdeswell, 2006). More recently Andreassen et al. (This volume) described a landform assemblage on the seafloor in upper Bjørnøyrenna, which they attributed to an episode of fast ice flow, followed by stagnation of the Bjørnøyrenna Ice Stream. We suggest that the stagnation features mapped and described in this study were formed during reoccurring periods of stagnation of the same ice stream.

3.1.4 Elongate and/or streamlined subglacial landforms

Several elongate landforms were mapped in Bjørnøyrenna (Figs. 2a, 3a). A striking example is shown in figure 2d (arrowed). It is needle-shaped with sharp, steep lateral edges and pointed upper and lower ends. The features are <40 km long, <500 m wide and <20 m high and occur on top of an ATB in northern Bjørnøyrenna (ice margin position 7; Figs. 2a, 3a). This ATB was overrun by readvancing ice which then stagnated as inferred from the occurrence of crevasse-squeeze ridges on the ATB surface and directly upstream of ice margin position 8 (Fig. 2a). Bottom reflections are visible in several chirp profiles, indicating that the elongate landforms are sedimentary features (Fig. 3b) formed at a later time than the ATB. We know of no previous examples of such landforms from published literature, and suggest that they be referred to as needles.

We are uncertain of the formational mechanism of the needles, but suggest that they may be related to the displacement of sediments by a combination of shearing and squeezing into longitudinal basal crevasses. The co-existence of crevasse-squeeze ridges, some of which have signs of longitudinal banding, and the needles (Fig. 2a) on the surface of the ATB indicates that these features are coeval and formed in relation to the aforementioned readvance. We suggest that the needles were formed immediately after stagnation of the ice stream snout, but before the upper part of the ice stream came to a complete halt. During such a setting, the stagnant snout may have provided a buttressing effect on the still advancing ice stream, which, in combination with the ice stream pushing from behind, raised the component of lateral extension (and longitudinal compression) to a level resulting in longitudinal crevassing and/or shearing. In other words, the distribution of crevasse-squeeze ridges and needles represents a shift from an extensional flow regime to a compressive flow regime, brought on by the great increase in backstress provided by the stagnant ice stream snout.

Other types of streamlined subglacial landforms have been described in previously published accounts from area 1. Andreassen et al. (This volume) described ~1.5 km wide and <10 m high groove-ridge features (north of ice margin position 9 in Figs. 2a, 3a), which they interpreted to be MSGLs formed by sediment deformation beneath a grounded ice stream. Solheim et al. (1990) described highly uniform and narrow (1-15 m) groove-ridge features with a relief of ~1 m (south of ice margin position 7 in Fig. 2a), which they interpreted to be glacial flutes. Furthermore, Rüther (2012) described streamlined seafloor (south of ice margin position 4 in Fig. 2a). Common for all of those features is that they are inferred to have been formed subglacially by fast-flowing grounded ice and the palaeo-ice flow direction may be inferred from them. We note with interest that we do not see clear evidence for streaming ice flow in the southern part of area 1 (Figs. 1, 2a). Clear MSGLs are seen in outer Bjørnøyrenna (Winsborrow et al., 2010), and upper Bjørnøyrenna (Rüther, 2012; Andreassen et al., This volume), but not in the southern part of area 1. It is possible that this is because of too limited data coverage or due to obliteration of MSGLs by stagnation features. Alternatively it may indicate that the ice did not stream in this area. More data are needed to establish this.

3.1.5 Iceberg ploughmarks, corrugated furrows and corrugation ridges

Several different types of seafloor furrows were mapped in the area. The first type is commonly observed in the shallower parts of the study area and are 2-5 m deep and 60-100 m wide furrows with a very sharp incision (Fig. 2e (arrowed)). Some of these furrows have a highly chaotic orientation, in some places going around in circles, while others are more unidirectional (Fig. 2e). These features have the characteristics of iceberg ploughmarks (Barnes and Lien, 1987) and are interpreted as such.

The second type is 2-4 m deep and 50-300 m wide furrows with a flat-bottomed incision. These features have a semi-trough parallel orientation, although their orientation may vary a bit laterally. Furrows of this type are not as common as the first type, they can extend up to 25 km and are observed on shallower ground within Bjørnøyrenna, such as on trough-transverse ridges. We also interpret these to be iceberg ploughmarks, however, we suggest that their flatter bases and greater width indicate formation by large, flat-bottomed icebergs discharged from a more proximal source and subsequent transport within a dense melange of icebergs which prevented them from turning.

Thirdly, furrows of highly uniform trough-parallel direction over a wide area were observed in association with proposed ice margin positions (Fig. 2b, e, g). They are best developed at three locations in Bjørnøyrenna (downstream from ice margin positions 2, 5-6 and 9 (Figs. 2a, 3a). In NW Bjørnøyrenna (downstream from ice margin position 9; Figs. 2a, 3a) they show a slightly larger degree of divergence. Furrows of this type are typically 70-200 m wide (but can be up to 500 m wide) and 2-20 m deep (Fig. 2b, e, g) and are interpreted to be ploughmarks incised by multi-keeled icebergs immediately downstream of the ice-front from which they originate. Some of these furrows contain numerous, uniform, parallel transverse ridges (Fig. 2b, e). The ridges are <2 m high, with a crest to crest spacing of 60-120 m. This is comparable with the dimensions of similar ridges previously described in Antarctic and Svalbard waters, referred to as a washboard pattern (Solheim and Pfirman, 1985; Barnes and Lien, 1987) or corrugation ridges within corrugated furrows (Jakobsson et al., 2011). Here we adopt the latter terms.

In general, iceberg ploughmarks in area 1 are oriented roughly parallel to Bjørnøyrenna. However, where area 1 and 2 overlap, two main orientations of ploughmarks were mapped. Ploughmarks on top of an ATB inferred to relate to retreat position 5-6 (Figs. 2a, 3a) are oriented parallel to the axis of Bjørnøyrenna. Meanwhile, ENE-WSW orientated furrows resembling either ploughmarks or ice-fingerprints are observed on a stratigraphically older surface, visible in NNW-SSE orientated depressions. Based on their stratigraphic location and uniform orientation they are inferred to be formed in close proximity to the ice margin during late stages of retreat from ice margin position 3 (Figs. 2a, 3a). The orientation of these furrows is consistent with input of ice from the small trough between Storbanken and Sentralbanken, hereafter referred to by the informal name Storbankrenna. The younger ploughmarks are more abundant and are oriented NNW-SSE, consistent with a source in upper Bjørnøyrenna (Figs. 1, 2a, 4a).

3.1.6 Ice sheet retreat in area 1

In area 1 the main ice flow direction is from N to S, parallel to the axis of Bjørnøyrenna, and later (in the northernmost part), from NW to SE, as inferred from the orientation of MSGLs (Fig. 2a). The occurrence of MSGL indicates that subglacial meltwater pressures were high enough to facilitate fast flow. An earlier event of ice flowing into Bjørnøyrenna from Storbankrenna (NE-SW) is also registered (Fig. 2a). The Bjørnøyrenna Ice Stream appears to have behaved in a very dynamic manner during its retreat which was characterised by several episodes of ice stream slowdown, stagnation, and reactivation as inferred from the nine identified ice margin positions (indicated by white numbers in Figs. 2a, 3a), with ice stagnation features associated with at least three of them (upstream of ice margin positions 3, 8 and 9 in Figs. 2a, 3a).

Several lines of evidence suggest that the Bjørnøyrenna Ice Stream experienced several episodes of retreat and readvance and that ice shelves formed in Bjørnøyrenna on at least three occasions. This evidence centres on the uniformly oriented multi-keeled iceberg ploughmarks in mid and upper Bjørnøyrenna (Fig. 2a, b, e, g) and landforms indicative of stagnation (crevasse squeeze ridges) downstream and upstream of these (Fig. 2a, c, f). Firstly, the excellent preservation of the relatively small crevasse squeeze ridges is hard to explain if retreat occurred primarily by calving. We therefore propose that after the crevasse-squeeze ridge networks were formed, the stagnant ice body floated off its bed, thereby forming an ice shelf. A similar formation mechanism is proposed for crevasse-squeeze ridge networks described by Andreassen et al. (This volume) in upper Bjørnøyrenna (upstream of ice margin position 9 in Fig. 2a). Secondly, we find it likely that the highly uniform furrows that occur in mid and upper Bjørnøyrenna (some of which are corrugated; Fig. 2a, b, e), were formed during times of increased ice flow velocities and calving rates (during ice margin positions 5 and 9; Fig. 2a, b, e), conditions known to occur subsequent to ice shelf break-up (Scambos et al. 2004). We further suggest that they were ploughed by mega-icebergs calved from the ice stream front, and held upright by an armada of icebergs. Tidal action on these large icebergs formed corrugation ridges, a process previously described in Antarctica by Jakobsson et al. (2011). Thirdly, the overall landform assemblage of stagnation features upstream from ice margin positions and downstream uniformly oriented mega-iceberg ploughmarks (Figs. 2a, c, f; 3) is consistent with ice stream acceleration induced by ice shelf break-up and followed by ice stream stagnation when the higher ice flow velocities could no longer be sustained.

The observed seafloor geomorphology of area 1 fits broadly with the model of episodic retreat presented by Ó Cofaigh et al. (2008) and Dowdeswell et al. (2008). However their model does not capture the repeated stagnation and ice shelf formation described here. A new model for ice stream retreat which includes ice stream stagnation (Andreassen et al., This volume), fits better in this setting. The cyclical behaviour (ice streaming, slowdown, stagnation and sometimes ice shelf formation) described in this paper provide an extension to both models, further suggesting that fast retreat between subsequent prolonged ice margin positions can occur primarily by float-off of stagnant ice and ice shelf formation rather than calving.

3.2 Area 2

Area 2 covers the Norwegian part of the 55 km wide, >100 km long (at 180-340 m bsl) Storbankrenna separating the shallower bank areas of Storbanken and Sentralbanken (Figs. 1, 4a). The underlying bedrock in area 2 consists of Mesozoic sedimentary rocks (Sigmond, 2002). Storbankrenna has previously been suggested as the source area for a chain of glacitectonic sediment blocks in Bjørnøyrenna (Rüther, 2012), implying that ice flowed from Storbankrenna into Bjørnøyrenna at some point.

3.2.1 Slope breaks, ridges and grounding zone wedges

The central part of area 2 is dominated by several large downstream pointing lobe-shaped ridges (10-20 m high and 3-10 km wide; indicated by white broken lines in Fig. 4a). The ridges resemble moraines, however, seismic data (Fig. 4g) reveal them to be bedrock features, covered by a relatively thin veneer (< 5 ms) of sediments (based on chirp data; Fig. 4f). In the eastern part of Storbankrenna the sediment cover is generally thicker (Fig. 4g), and four slightly curved, steep ridges made up of acoustically semi-transparent sediments (10-20 ms thick, 1.2-5 km wide and 10-20 km long) have been identified (Fig. 4a; arrowed in 4f, g). Solheim et al. (1990) mapped an elongate accumulation of sediment (between 10-20 ms thick) in the northern middle part of Storbankrenna and interpreted it as till or moraine material. This accumulation appears to be the northwest continuation of one of the described ridges, which we interpret to be recessional moraines representing marginal positions during slow retreat of the ice sheet (indicated by black lines in Fig. 4a). The chirp/seismic data (Fig. 4f, g) also show that a marked break in slope in the eastern most part of area 2 (Fig. 4a), coincides with the downstream end of a thick (>20 ms) ATB, in the area where the seafloor is generally smoother. We interpret a hummocky reflection within the ATBs convex front, to represent a recessional ridge (4f, g). In the northern part of this accumulation, streamlining of the seafloor was observed (Fig. 4a). The linear features trend NE-SW and are ~4 m high and 400-600 m wide and we interpret them to be MSGLs indicative of fast ice flow (Stokes and Clark, 1999, 2001). Based on the arguments described in chapter 3.1.1 we suggest that the ATB is a grounding zone wedge, and thereby represents a former ice marginal position, with the southwestern end of the streamlining indicating the location of the ice extent in the northern part (Fig. 4a). The location of the ice margin in the eastern and southern sectors of area 2 is unknown.

3.2.2 Ice-fingerprints and ploughmarks

Other indications of ice retreat across Storbankrenna include features that closely resemble the ice-fingerprints described in chapter 3.1.2. They form several km-long, more or less linear chains of ridges (Fig. 4b, d). The ridges are 60-600 m wide and 1-12 m high, have a crescentic shape, with the ends pointing upstream and with flat-based 380-2500 m long and 100-700 m wide depressions between them, oriented normal to the ridges (Fig. 4b, d). Analysis of chirp data shows that the ridges are unlithified sediments (Fig. 4c, e), and we interpret them to be berms of ice-fingerprints. We believe that where the ice-fingerprints form unbroken chains they represent former ice margin positions and that they were formed during slow retreat of the ice sheet from Bjørnøyrenna across Storbankrenna. However, we cannot rule out that some of the ice-fingerprints occurring in shallower areas or not forming ridge chains, may be iceberg-pushed ridges.

A number of seabed furrows are observed in area 2 (Fig. 4a). The furrows are 3-7 m deep and 70-400 m wide and can be either flat-based or more angularly incised, and in some cases have berms along them. In the eastern part of area 2 examples of several highly parallel furrows crossing other sets of highly parallel furrows are observed. The majority of the furrows are oriented roughly NE-SW along the long axis of the valley or N-S/NW-SE. An exception to this occurs in the westernmost part as previously described in chapter 3.1.5. The NE-SW oriented furrows are interpreted to be iceberg ploughmarks originating from icebergs calved off the ice margin retreating across area 2 (from SW to NE), where the highly parallel furrows are interpreted to be incised by multi-keeled icebergs. Ploughmarks oriented in a more N-S direction are interpreted to originate from an ice margin in Bjørnøyrenna.

3.2.3 Ice sheet retreat in area 2

In this area two main ice flow directions are inferred: NW-SE in the western part of Storbankrenna and ENE-WSW in the remaining parts of the trough. Based on the successive chains of ice-fingerprints, we infer that ice retreated slowly from Bjørnøyrenna towards the NNE/NE up onto Storbanken and towards the ENE across Storbankrenna, with several ice margin retreat positions. In the innermost part of the valley, the occurrence of MSGLs on a GZW is interpreted to represent a switch in ice flow regime with an increase in basal meltwater pressures, leading to faster ice flow and possibly increasing the role of deposition from glacial meltwater (see also chapter 4.3).

3.3 Area 3

This area (Figs. 1, 5a) covers the Norwegian part of the relatively shallow Storbanken (95-250 m bsl), an area where the bedrock consists of Mesozoic sedimentary rocks (Sigmond, 2002). Several thick accumulations of glacigenic sediment (Fig. 5a) interpreted to be till and/or moraine complexes have been identified in area 3 (Elverhøi and Solheim, 1983; Solheim and Kristoffersen, 1984). Furthermore, several studies have concluded that a large ice divide was centred on Storbanken-Kong Karls Land during the Late Weichselian glaciation (Lambeck, 1995, 1996; Bondevik et al. 1995; Forman et al., 1995; Landvik et al., 1998; Ottesen et al., 2005).

3.3.1 Slope breaks, ridges and sediment thickness

Several large ridges are easily identified on the IBCAO v.3 and Olex datasets (Fig. 5a). They range in dimensions from 10-25 m high, 2-15 km wide and up to 100 km long. The westernmost ridges consist of up to more than 30 ms thick glacigenic sediments previously interpreted to be moraines (Elverhøi and Solheim, 1983; Kristoffersen et al., 1984; Solheim et al., 1990). We agree with this interpretation, which implies that they were deposited during a prolonged stillstand of the ice sheet margin. We tentatively suggest that the remaining mapped ridges (Fig. 5a) may also be moraines, representing positions where the ice sheet halted for a considerable time during overall retreat, although this interpretation remains to be verified. No ATBs were identified on the seafloor or subsurface data, perhaps suggesting a different glacidynamic setting in area 3 from that in the troughs (area 1).

3.3.2 Small curvilinear ridges, ice-fingerprints and ploughmarks

Small ridges (2-5 m high, 40-200 m wide) are observed west of, and in between, the large moraines but not superimposed on them (Fig. 5b, c, d). They have a semi-transparent acoustic character and form a network of successive lobate or curvilinear ridges that stretch over at least 5-10 km. We interpret the ridge to be retreat moraines formed by ice push, possibly during small winter advances of the ice margin (Boulton, 1986). Recessional moraines of this type are associated with slow, steady ice retreat (Ottesen and Dowdeswell 2006, 2009). Here, if each ridge represents one winter advance it would have taken the margin ~50 years to retreat across the area in Fig. 5c, at an average retreat rate of about 100-150 m/year.

In deeper areas or small basins within the ridge networks, depressions with crescentic fronting ridges interpreted to be ice-fingerprints occur (fig 5c, arrowed). The crescentic or convex-downstream shaped ridges or berms are 60-100 m wide and 1-5 m high and the depressions between their upstream ends are 200-250 m wide.

Furrows in shallower parts of area 3 are mostly 1-6 m deep and 40-250 m wide, have a pointed or flat bottom and either uniform or chaotic orientations. These are interpreted to be iceberg ploughmarks which may have travelled some distance, although some of the more uniformly oriented (NNE to SSW), flat-bottomed ploughmarks may have been formed in close proximity to an ice margin.

3.3.3 Ice sheet retreat in area 3

Based on the orientation of the westernmost small recessional ridges (Fig. 5b, c) we suggest The in area 3 the main ice flow direction during early deglaciation was from N-S . During this phase ice retreat was slow and steady at a rate of 100-150 m/year assuming the ridges were formed annually. During a later phase, the slow and steady ice retreat was repeatedly punctuated by prolonged periods of ice margin still-stand during which large moraines were deposited. This later phase was characterised by ice flow from ENE, E or ESE, as inferred from the orientation of the large moraines and the small retreat ridges (Fig. 5a), reflecting a change from a regional ice divide on Storbanken to a smaller local dome.

3.4 Area 4

This area encompasses the eastern part of Sentralbanken, the northern part of Thor Iversen-banken and the trough between these banks, referred to here by the informal name Sentralbankrenna (Figs. 1, 6a). The western extension of Sentralbankrenna, which makes up the southeast “heel” of Bjørnøyrenna, is also part of this area (Figs.1, 6a). Depths in area 4 range from 120-440 m bsl and the underlying bedrock consists of Mesozoic sedimentary rocks along with small occurrences of Upper Palaeozoic salt (Sigmond, 2002). Based on the large scale bathymetry of the central Barents Sea it has been suggested that Late Weichselian ice flowed from Sentralbankrenna towards Bjørnøyrenna (Landvik et al., 1998; Ottesen et al., 2005). The distribution of tunnel valleys and retreat ridges in Sentralbankrenna, indicates that warm-based ice occupied the valley and that drainage was channelised during late retreat stages (Bjarnadóttir et al., 2012).

3.4.1 Description and interpretation of geomorphic features

A major slope break and two ridges (6-8 km wide, 10-15 m high, up to 30 km long) were mapped west of 30° E (Fig. 6a). We have no subsurface data from this area and cannot conclude on whether they are bedrock or sediment features. A pronounced slope break (oriented W-E) was identified at the point where Bjørnøyrenna opens up into Sentralbankrenna (centre at 30° E). We are not able to confidently conclude upon the origin of this slope break, although available seismic data indicates a bedrock boundary, suggesting that it is not related to ice retreat. Two distinct slope breaks mapped east of 30° E (Fig. 6a), are characterised by a steep, convex rise of the seafloor towards the east. Seismic and chirp data reveal them to be large accumulations of acoustically transparent sediment, making up four ATBs (Fig. 7a, b). They are numbered from 1-4 in stratigraphic order from bottom up (Fig. 7b). The ATBs are separated from the underlying sedimentary bedrock by an erosional unconformity (Fig. 7a).

ATB1 is ~20 ms thick. As we do not have data to define its western boundary, we cannot delimit its spatial distribution (Fig. 7b). ATB2 laps onto the eastern part of ATB1, is ~20-30 ms thick in the front but much thinner (<10 ms) where ATB3 laps onto it (Fig. 7b). We are only able to follow the ATB2 unit for ~25 km upstream due to loss of chirp signal penetration when sediment thickness exceeds ~40 ms (Fig. 7b). ATB3 has a rather flat surface, is up to 50 ms thick (Fig. 7a, b) and continues ~30 km towards the east (Fig. 7a), where the sediment has a semi-transparent acoustic character with a few faint reflection segments and a more hummocky upper surface (Fig. 7a). Uppermost is ATB4 which is the thickest, reaching up to 70 ms (Fig. 7a). It has a steep, convex front and the unit is as a whole smoothly convex (Fig. 7a). It continues ~80 km to the east and terminates at an east-west oriented slope break immediately northeast of the eastern part of ATB4 (Figs. 6a, 7a). The large-scale geomorphology indicates that the ATB continues southwards to the Thor Iversen-banken (Fig. 6a), and is even wider there. On the seafloor at the easternmost part of ATB4, linear groove-ridge features with a NE-SW orientation were mapped (Fig. 6b, c). These features have a relief of up to 8 m, are 200-800 m wide, 12 km long and are formed in the ATB sediment. The dimensions and elongation ratio (1:15-60) of these features indicate that they are mega scale glacial lineations (MSGLs) according to criteria of Stokes and Clark (1999, 2001). MSGLs are believed to be formed by sediment deformation beneath fast-flowing ice streams (Alley et al., 1986), ploughing by ice keels (Clark et al., 2003) or a combination of the two (Wellner et al., 2006). We suggest that the described ATBs in area 4 represent GZWs deposited primarily from glacial meltwater emerging at the margin of an ice stream occupying Sentralbankrenna, with additional input from other grounding line processes (as described in chapter 3.1.1). The GZW wedges are numbered according to their ATB number. For GZWs 1-2 we propose that the ice margin was located where the GZWs pinch out in the eastern, upstream end (Fig. 7b). We suggest that when GZW3 was formed the ice margin was located where the acoustic characteristics of the deposit change, and that the eastern part with the hummocky surface was deposited subglacially and modified by ice-push and possibly meltwater erosion during retreat of the margin. We propose that when GZW4 was deposited, the ice margin was located at the western termination of the MSGLs (Fig. 6b).

The next mapped slope break to the northeast (Fig. 6a,b) may be a former ice margin position, but it is not possible to confirm that this is a separate GZW based on the seismic data . Similarly, no MSGLs were identified directly upstream from this GZW. However, it is possible such features may have been obliterated by iceberg ploughing as ice retreated over the area. Here, and towards the next mapped slope break to the NE, the seafloor is characterised by < 3 m deep and <200 m wide curvilinear furrows with angular incisions and < 1 m high berms. The furrows are of quite uniform orientation in the northeastern most part of this area (Fig. 6b, d), but diverge to the SW. We interpret the furrows to be iceberg ploughmarks carved by icebergs proximal to the ice margin.

Farther to the northeast, the next mapped slope break (transverse to line c in Fig. 6a), coincides with an ice margin deposit identified by Bjarnadóttir et al. (2012). Seismic/chirp data (Fig. 7c) show that the main break in slope is controlled by a bedrock protrusion and that there is an ATB downstream (Fig. 7c, d). Upstream from this ATB, groove-ridges features are observed on the seafloor. They have a uniform NE-SW orientation, are ~300 m wide with flat bottoms and have a relief of 1-2 m. These features are more uniformly oriented than the inferred ploughmarks immediately downstream of the ATB. We interpret the groove-ridge features to be MSGLs and the ATB to be a GZW. We therefore argue that this slope break represents an ice margin position and suggest the bedrock protrusion served as a pinning point.

The remaining mapped features in area 4 are ridges. To the southeast they are oriented roughly N-S and several of these have been confirmed to consist of acoustically semi-transparent sediment (Bjarnadóttir et al., 2012). We find it likely that the remaining ridges on the flank of Thor Iversen-banken are also sedimentary (Fig. 6a, b). Mapped ridge features in the northern part of area 4 are oriented NE-SW. Several of these ridges are made up of acoustically semi-transparent sediment according to Bjarnadóttir et al. (2012), and a seismic profile across two of the mapped ridges confirms that they are sedimentary and up to 20-35 ms thick (Fig. 7e). We find it likely that all the mapped features in the northern part of area 4 are sediment ridges, but further data are needed to verify that. Considering the large size of the ridges and the distance between them (several km), we do not think these are annual ridges but interpret them to be recessional moraines formed at successive prolonged ice margin stillstand positions and indicative of slow ice retreat

Elverhøi and Solheim (1983) mapped glacial sediments of unknown thickness over a large area of Sentralbanken (Fig. 6a). They state that this sediment was overrun by glacier ice, but are unsure whether it is subglacial or glacimarine in origin. We do not have information about seabed morphology or thickness of the accumulation so cannot conclude whether it is related to an ice margin position, however, comparison with other large sediment accumulations in this part of the Barents Sea suggests that this is likely.

Many parts of the seabed in area 4 are heavily furrowed (Fig. 6b, d). The furrows are 1-5 m deep and 50-400 m wide and in the eastern part of Sentralbankrenna they have a highly uniform NE-SW orientation (Fig. 6b, d). Although the seabed furrows are more chaotically oriented in the remaining parts of area 4, the majority are oriented N-S in the shallower northern part, SE-NW in the southern part and ESE-WNW in the middle and western part (Fig. 6a). These seabed furrows are interpreted to be iceberg ploughmarks. The uniform ploughmarks (Fig. 6d) are attributed to ploughing by icebergs proximal to an ice front which they calved from (forming the GZW farthest to the northeast), while the more chaotically arranged ploughmarks are inferred to have been ploughed by icebergs in a more ice-distal location.

3.4.2 Ice sheet retreat in area 4

In Sentralbankrenna the main ice flow direction was from ENE to WSW in the early stages of deglaciation. In the central part of the area there is evidence of at least five ice margin positions associated with deposition of GZWs, which combined with MSGLs indicate a dynamic ice stream supported by high basal meltwater pressures occupied Sentralbankrenna at the time. Later the ice retreat appears to have been slower and successive large retreat moraines were formed during prolonged stillstands of the ice margin. At the same time the ice flow direction became more topographically controlled, with ice flow from the northwest in the northern part (on Sentralbanken), from the east in the eastern part and from the southeast in the southern part (on Thor Iversen-banken).

3.5 Area 5

This area covers Thor Iversen-banken, Tiddlybanken and the northern part of Murmanskbanken (Figs. 1, 8a). Depths in the area range from 320-165 m bsl and the underlying bedrock consists of Mesozoic sedimentary rocks and Upper Palaeozoic salt in the northwest part (Sigmond, 2002). According to Epshtein et al. (2011a) the southern part of area 5 is covered by over-consolidated till. An exception to this is the large Murmanskbanken ATB which is normally consolidated and which they attribute to subglacial deposition in interior parts of the Barents Sea Ice Sheet. Svendsen et al. (2004) on the other hand, interpreted the sediments to be a sequence of moraines deposited on Murmanskbanken by ice flowing from Sentraldjupet.

3.5.1 Description and interpretation of geomorphic features

Several seafloor ridges and one major slope break were mapped based on IBCAO v3 and Olex (Fig. 8a). The majority of the ridges are oriented in a NNW-SSE direction with local changes to a more WNW-ESE direction. The ridges are 7-18 km wide, <45 m high, 19-160 km long and have a is convex and sometimes hummocky surface (Fig. 8a). Where sparker data are available they show that the ridges consist of >20 ms thick acoustically semi-transparent sediments with internal reflection segments, overlying an erosional unconformity (Fig. 8b, c). No indications of fast ice flow such as streamlining or MSGLs were observed in relation to the ridges. We interpret the sediment ridges to be moraines, pushed up at the margin of an ice sheet during temporary stillstands in times of overall slow retreat.

The mapped slope break stretches from the middle of area 5 to its southern end in a N-S and NW-SE direction (Fig. 8a). Sparker data (Fig. 8d, e) shows that the slope break marks the western termination of an up to 50 ms thick acoustically transparent sediment body (Fig. 8d, e). The front of the ATB is steep and convex, while its lower boundary and surface is only slightly convex or almost flat (Fig. 8d, e). In the southern part of area 5 the ATB laps down onto another acoustically transparent unit (inset in Fig. 8e). The extent of the lower unit (ATB1) is not known, but the upper unit (ATB2) extends as a ~100 km broad belt across the area.

The ATBs (1 & 2) in area 5, have previously been described and mapped by Epshtein et al. (2011a, b). Their mapping includes the southernmost part of the ATB and extends further south than that of this study. We extend their mapping of ATB2 in the northern end, and propose a different interpretation. Epshtein et al. (2011a, b) described ATB2 sediments as normally consolidated sandy mud and interpreted it to consist of till formed beneath the interior parts of the ice sheet during conditions of excessive melting and note the similarities between the ATB sediments and that described from beneath ice streams in Antarctica. They describe the surface of ATB2 as wavy in places and interpret the waves to be MSGLs oriented transverse to the eastern boundary of ATB2 (Epshtein et al., 2011a). In our opinion a more likely explanation is that ATB2 is a grounding zone wedge (non-generic sense) deposited at the margin of streaming ice (as inferred from the MSGLs). We suggest it was formed largely through deposition from glacial meltwater plumes emerging at the margin along with other grounding line processes (see chapter 3.1.1) and melting from the basal layer in the grounding zone. This is the same process suggested for the formation of GZWs in areas 1, 2 and 4, and similar to descriptions of similar deposits from other locations in the Barents Sea

(Elverhøi and Solheim, 1983; Kristoffersen et al., 1984; Solheim and Pfirman, 1985; Solheim et al., 1990; Bjarnadóttir et al., 2013).

The seafloor in area 5 is heavily dissected by furrows (simplified directions are shown in Fig. 8a). The furrows are 3-10 m deep and 50-200 m wide, some have flat bottoms while the majority of them do not. Berms (~1 m high) on one side or both are sometimes observed. We interpret the furrows as iceberg ploughmarks. In area 5 most of the ploughmarks are fairly straight, while the rest are oriented in a more chaotic manner. The main ploughmarks are oriented ENE-WNW and SE-NW, and we suggest that after icebergs calved off the ice margin during respective stillstand positions they drifted in a northwest direction.

3.5.2 Ice sheet retreat in area 5

In area 5 several retreat positions were identified. The earliest ice flow event mapped here was from ENE, ice retreat was slow and moraine ridges were formed during stillstands. According to Bjarnadóttir et al. (2012) the moraines are cut in several places by meltwater channels, indicating an effective channelised subglacial meltwater drainage system was active during their formation. The effective drainage configuration may have resulted in relatively low subglacial meltwater pressures and high yield strengths of subglacial sediments (Piotrowski et al., 2004), which can explain the different acoustic character of the moraines as compared to GSWs (see also chapter 4.3). Later, a large GZW was deposited from a leaky ice margin along the apex of Murmanskbanken. The general ice flow direction was from E-W, ENE-WSW or ENE-WSW, suggesting the area was overrun by ice flowing in from the east.

4 Ice sheet configuration and behaviour during deglaciation

In this section we present and discuss a new reconstruction of the deglaciation of the central Barents Sea (Fig. 9) based on the findings from areas 1-5. In the reconstruction we identify changes in predominant ice flow directions, several new ice sheet retreat stages, areas characterised by dynamic ice associated with episodic retreat (sometimes involving stagnation and ice shelf formation), and areas characterised by more sluggish ice associated with slower retreat (Fig. 9).

4.1 Palaeo-ice flow directions

Palaeo-ice flow directions from two main source areas were registered for areas 1-3 (Storbanken, Storbankrenna, Bjørnøyrenna; Fig. 9). Older iceberg ploughmarks and ice-fingerprints mapped in area 2 indicate an early phase of ice flowing into Bjørnøyrenna from the northeast through Storbankrenna (Fig. 9). This ice flow direction has previously been documented by chains of glacial rafts and glacial lineations (Rüther, 2012). In Bjørnøyrenna (NW of Storbankrenna), the orientation of subglacial landforms (this study and Andreassen et al., This volume) indicates that ice flow directions gradually shifted from a NE-SW direction, to a N-S and later NW-SE orientation (Fig. 9). We suggest this reflects a gradual shift of source area through ice divide migration, with an increasingly large portion of ice input from the northern Svalbard area rather than from the east (Fig. 9). This is consistent with previously published reconstructions based on glacial geological mapping onshore and offshore and isostatic inversion models, indicating ice divides centred over Storbanken-Kong Karls Land (Bondevik et al., 1995; Salvigsen et al., 1995; Lambeck, 1996; Landvik et al., 1998; Ottesen et al., 2005; Fig. 9), between Kong Karls Land and Nordaustlandet (Salvigsen et al., 1995) and southern Hinlopenstretet (Dowdeswell et al., 2010; Fig. 9). We suggest that the first was the main ice divide during the Last Glacial Maximum (LGM) and early deglaciation, while the latter two were short-lived positions towards the end of deglaciation, at which time a much reduced dome persisted on Storbanken (as indicated by the distribution of recessional ridges). The timing of deglaciation in areas 1-3 is constrained by a date of 16.9-17.5 cal ka close to the shelf break (Fig. 9; Rüther et al. 2011), and raised beaches on Kong Karls Land dated to 11.1-11.6 cal ka inferred to be formed after complete deglaciation of the areas (Fig. 9; Salvigsen, 1981). However, we wish to emphasise that the older and younger phase may not have been synchronous in all areas and that better age control is needed in order to pinpoint the timing of different phases during retreat.

During the early phase of ice retreat across areas 4-5 (Sentralbanken, Sentralbankrenna, Thor Iversen-banken, Murmanskbanken; Fig. 9) palaeo ice flow was from ENE, based on the orientation of inferred grounding line deposits and MSGLs (early phase in Fig. 9). This confirms previously suggested ice flow patterns in the Sentralbanken-Murmanskbanken region, based on large-scale bathymetry (e.g. Landvik et al. 1998; Svendsen et al., 2004; Ottesen et al., 2005). Ice flow became increasingly topographically influenced over the shallower bank areas during a later phase of ice retreat in the area (Fig. 9), suggesting development of local ice divides over Sentralbanken and Thor Iversenbanken as deglaciation advanced. The timing of deglaciation in areas 4-5 is constrained by radiocarbon dates from glacimarine sediments of 16.9-17.5 cal ka near the continental shelf break (Fig. 9; Rüther et al. 2011) and 14.2-15.6 cal ka in Sentraldjupet (Polyak et al. 1995).

4.2 Glacial dynamics

In the ice sheet retreat reconstruction (Fig. 9) we have adopted and modified palaeo-ice margin positions in Bjørnøyrenna suggested by Rüther (2012) and Andreassen et al. (This volume). Furthermore, we have extended the Murmanskbanken line of Svendsen et al. (2004). We additionally propose several new retreat stages in all areas (Fig. 9), and map cross-trough bedrock protrusions as possible ice pinning-points during retreat.

Based on the distribution of overridden GZWs and crevasse-squeeze ridge networks, we have identified at least two major readvances in Bjørnøyrenna (ice margin positions 1 and 7 in Fig. 9) and three events of ice stream stagnation (related to ice margin positions 3, 8 and 9 in Fig. 9). Bjørnøyrenna (area 1) was occupied by a highly dynamic ice stream, which experienced several cycles of fast ice streaming, slowdown and stagnation, followed by reactivation and readvance. Based on the distribution of retreat ridges in the bank areas flanking Bjørnøyrenna (areas 1-3; Figs. 2, 3, 4, 5, 9), we suggest that ice retreat there was slower. An exception to this is found in the eastern part of Storbankrenna (area 2; Figs. 4, 9) where a GZW has been mapped. In area 4, the occurrence of MSGLs and GZWs in Sentralbankrenna suggest an early phase dominated by dynamic conditions with fast ice flow and episodic retreat. Meanwhile, retreat ridges and a lack of fast flow indicators in the shallower parts of area 4 suggest a later phase characterised by slow ice retreat. In area 5, the opposite holds true, with an early phase characterised by moraine formation (slow retreat) and the later formation of a large GZW characteristic of a more dynamic regime.

4.3 Controls on cyclical behaviour and type of ice margin deposit

Geomorphic features on buried surfaces indicate that the Bjørnøyrenna Ice Stream experienced oscillations between active and quiescent periods during pre-LGM glaciations (Andreassen and Winsborrow, 2009). Similarly, a shift from cold-based conditions during early deglaciation (characterised by compressional flow), to warm-based conditions when deglaciation was well underway (characterised by extensional flow), has been inferred to have taken place during the last deglaciation in Bjørnøyrenna (Rüther, 2012). The data presented in this paper suggest that during the last deglaciation the Bjørnøyrenna Ice Stream went through not only one, but reoccurring cycles of fast streaming ice flow and slower flow. The results further indicate that slowdown may, in some cases, have been followed by ice stream stagnation (sometimes leading to floating-off and ice shelf formation), before ice streaming was reinitiated (Fig. 10). What drove the observed ice flow cycles is uncertain. In Bjørnøyrenna we propose that ice shelf break-up might have induced rapid ice acceleration, however, what triggered the velocity changes in other areas where evidence for ice shelves is not seen. Andreassen and Winsborrow (2009) favoured till stiffening due to freezing during pre-LGM glacial maxima), but also mentioned dewatering as a possible mechanism. Within the study area we have seen differences in grounding line deposits which we believe are associated with different ice velocity and meltwater regimes. We will now explore how variations in meltwater availability, drainage configuration and substrate drainage capacity may have influenced ice velocity in the central Barents Sea.

In the central Barents Sea, ice margin positions are marked by either large GZWs made up of acoustically transparent sediments or moraine ridges consisting of acoustically semi-transparent sediments with internal reflection segments. Similar to the conclusions of other studies (e.g. Solheim and Pfirman, 1985; Solheim et al. 1990; Ottesen and Dowdeswell, 2006), we suggest that GZWs are typical grounding line deposits in areas of warm-based dynamic ice, whilst the moraines are associated with slower retreat of more sluggish ice.

Bjarnadóttir (2012) suggested that the maturity (efficiency) of the subglacial meltwater drainage network is directly related to both whether a GZW or a moraine is formed at prolonged ice margin positions, and the geometry of GZWs. In light of the observed cyclical behaviour of the Bjørnøyrenna Ice Stream we want to extend this idea and suggest that the type of grounding line deposit formed also reflects the relative abundance of subglacial meltwater, which in turn governs the type and maturity of subglacial drainage system. How subglacial sediments react to different amounts of subglacial meltwater is influenced by the amount of meltwater, the permeability of the subglacial sediment and basal thermal regime (Piotrowski et al., 2004), meaning that both local and regional conditions can influence the state of the subglacial sediments and drainage system. In general, there seems to be a very sensitive balance between which type of drainage style is dominant and changes from one type to the other may be rapid (Smith et al., 2007; Hubbard et al., 1995). Thus, a sudden increase or decrease in meltwater abundance could lead to a change in the meltwater drainage organisation and potentially also the type of grounding line deposition.

To develop this idea further, we consider area 5. Here, retreat ridges are breached by subglacial meltwater channels (Bjarnadóttir et al., 2012), implying channelised and effective drainage of subglacial meltwater to the margin at the time of their formation. Conversely, no such meltwater channels are observed in association with the large Murmanskbanken GZW (Fig. 8a), implying a switch in the type of drainage system. We suggest that the channelised system active during moraine formation and subsequent retreat, gradually closed leading to increased basal meltwater pressure and a change back to a distributed drainage system. Such a switch could have led to increased subglacial meltwater pressures resulting in the formation of soft (dilated) till and the reinitiation of ice-streaming (Smith et al., 2007). This fits well with the proposed formational mechanism of the Murmanskbanken GZW, where deposition from meltwater plumes escaping along a leaky margin (cf. Powell and Alley, 1997) .

Switching in subglacial drainage systems may also explain the differences in the acoustic characteristic of the different grounding zone deposits (GZWs and large retreat moraines). The semi-transparent moraine sediments would be expected to represent well-drained, heterogenous sediments with yield strengths exceeding pore-water pressure (stiff system). Meanwhile the ATB sediments would be expected to represent more homogenous, less effectively drained sediments with low yield strengths (saturated system).

The ATBs identified in this study have been interpreted to be GZWs and bear many similarities to those deposited in the grounding zone of fast-flowing ice streams (e.g Powell and Alley, 1997; Dowdeswell and Fugelli, 2012, Livingstone et al., 2012, and references therein). However, there are some important differences. The ATBs are not truly wedge-shaped, and may instead be of quite continuous or varying thickness, and be lense- or ridge-shaped and tend to fill up depressions. They are also thinner than the majority of GZWs (Dowdeswell and Fugelli, 2012). Their acoustic signature is limited to acoustically transparent sediments, with very few internal horizontal reflections. This differs from descriptions of GZWs whose acoustic signature includes dipping internal reflections truncated by a more horizontal reflection, and overlain by a unit of acoustically transparent sediments which may or may not contain gently dipping internal reflections. The dipping reflectors are considered to correspond to prograding foresets deposited by sediment gravity flows, while the acoustically transparent unit has been interpreted as topsets formed by the deposition of deforming basal till (e.g. Powell and Alley, 1997; Livingstone et al. 2012). A recent study of GZWs on the continental shelf of Greenland revealed that this pattern can be even more complex, suggesting that different processes can contribute to the formation of GZWs at different times, resulting in a variance in appearance (Dowdeswell and Fugelli, 2012).

Powell and Alley (1997), suggested that GZWs form at polar shelves void of meltwater, and represent one end-member on a continuum of grounding zone deposit types, with morainal banks being the end-member associated with ice margins with more meltwater. Between these two end-members it is likely that there exist several types characterised by varying importance of different grounding line processes such as pushing, squeezing and lodgement of sediments, as well as deposition from meltwater, iceberg rainout and through calve-dumping (Powell and Alley, 1997). Therefore, the more varied acoustic character of some of the Greenland GZWs described by Dowdeswell and Fugelli (2012), may indicate that they are more intermediate types of GZWs. Similarly, we find it most likely that the GZWs in the Barents Sea represent another intermediate stage closer to the meltwater-end of the continuum.

4.4 Parallels with the West Antarctic Ice Sheet

There are many parallels between the palaeo- Barents Sea Ice Sheet and the West Antarctic Ice Sheet such as their setting (marine-based on shallow continental shelves, underlying sedimentary bedrock, high-latitude location), LGM-size (Mercer 1970; Siegert et al. 2002; Andreassen and Winsborrow, 2009) and palaeo-records from the continental shelves (Livingstone et al. 2012 and references therein). Furthermore, there are many similarities between the observed and modelled behaviour of these ice sheets. Firstly, evidence indicates that West Antarctic ice streams are prone to both small and large scale dynamic adjustments and several papers describe examples of ice streams that have experienced slow-down, stagnation, reactivation and flow-switching (Retzlaff and Bentley, 1993; Anandakrishnan et al., 2001; Joughin et al., 2002; Joughin and Tulaczyk, 2002; Hulbe and Fahnestock, 2007) due to meltwater-rerouting, ice-piracy and/or basal temperature changes (Bennett 2003; Bougamont et al., 2003; Hulbe and Fahnestock, 2007). Secondly, the presence and motion of subglacial meltwater at the onsets and beds of several Antarctic ice streams have been documented (Fricker et al. 2007; Bell 2008; Smith et al. 2009), and are known to locally influence ice flow velocity and surface elevation leading to dynamic readjustments (Bell 2008; Stearns et al., 2008). Thirdly, the episodic and/or slow retreat pattern observed in the Barents Sea is similar to that of several Antarctic palaeo-ice streams (e.g. Livingstone et al. 2012 and references therein). Finally, the Western Divide in West Antarctica has recently been observed to migrate in response to dynamic drawdown (Conway and Rasmussen, 2009).

These examples from West Antarctica are similar to conclusions from SW Barents Sea indicating that ice divides migrated due to dynamic readjustments (Andreassen et al., This volume; This paper), that the ice streams experience shifts between ice stream slowdown/quiescence and reactivation/fast ice stream flow (e.g. Andreassen et al., 2007; Andreassen and Winsborrow, 2009; Rüther et al. 2011; Andreassen et al., This paper), and that meltwater frequently existed at the ice sheet bed (Bjarnadóttir et al., 2012; Bjarnadóttir et al., 2013). One major difference is that we propose that during the later phase of deglaciation in the Barents Sea, the relative abundance of subglacial meltwater may have had a greater influence on the dynamic response of ice streams, a condition which may not yet have been reached by Antarctic ice streams.

Changes in the abundance of basal meltwater and cycles of ice flow velocity may also reflect longer term changes brought about by external forcing factors such as climatic warming. This is likely to have been especially significant, if, as suggested, ice shelves developed in Bjørnøyrenna during deglaciation, as Antarctic examples have demonstrated the high sensitivity of ice shelves to increased surface melt (Scambos et al., 2003), warming oceans (Payne et al., 2004; Bindschadler, 2006) and/or sea level rise (Jakobsson et al., 2011). Furthermore, in Antarctica the loss of a buttressing ice shelf has led to reactivation and speed-up of ice streams (De Angelis and Skvarca, 2003; Rignot et al., 2004; Scambos et al., 2004). This scenario closely resembles the repeated cycles of fast ice stream flow and stagnancy observed in Bjørnøyrenna, and further work should be done to address whether and how such forcing factors influenced deglaciation of the central Barents Sea.

5 Conclusions

This paper presents results based on several new marine geophysical datasets from the central Barents Sea. The results were combined with previously published data to produce a new reconstruction of deglaciation in the central Barents Sea. These new conclusions significantly advance the knowledge and understanding of the configuration and dynamics of the Barents Sea Ice Sheet during its last retreat across the study area. In Bjørnøyrenna-Storbanken (areas 1-3) there was a strong input of ice from NE and N during an early phase of deglaciation. Ice flow shifted to a NW source area during later stages of deglaciation in Bjørnøyrenna, and became more topographically controlled on adjacent bank areas. Farther south (in areas 4-5) ice came mainly from NE, but was more influenced by local topography during later stages of deglaciation. Different styles of retreat are seen in the central Barents Sea during early and late phases of deglaciation. Within Bjørnøyrenna (area 1) the ice was highly dynamic, with repeated cycles of ice streaming and stagnation occurring throughout deglaciation (resulting in ice shelf formation and episodic ice retreat). In Storbanken-Storbankrenna (areas 2-3) the ice was more sluggish and retreat was slower than in Bjørnøyrenna, apart from a late phase characterised by fast ice flow in eastern Storbankrenna. In the area between Sentralbanken and Thor Iversen-banken (area 4), the early phase was characterised by fast flowing ice and episodic retreat, while the later phase was characterised by slow retreat and topographically controlled ice flow. On Thor Iversen-banken and Tiddlybanken (areas 4-5) ice flow was comparatively sluggish and retreat slower throughout deglaciation, while Murmanskbanken (area 5) appears to have been occupied by fast flowing ice during the later phase. We suggest the observed cyclical behaviour and shifting ice flow dynamics, along with the different types of ice marginal deposits, is governed by the availability of meltwater at the ice-bed interface, the drainage capacity of the substrate and the stabilising forces acting on the ice (for example the buttressing effect of an ice shelf). Similar cycles of ice flow velocity have been observed and modelled in West Antarctic ice streams, however here the glacial cycle has not reached the point where subglacial meltwater abundance becomes the dominant control on the dynamic response of ice streams as we observe in Bjørnøyrenna.

Acknowledgements

We acknowledge the PhD Trainee School in Arctic Marine Geology and Geophysics (AMGG) at the University of Tromsø for funding LRB, and the Research Council of Norway (NFR), Det Norske ASA, Statoil and BG group Norway for funding the PetroMaks project "Glaciations in the Barents Sea area (GlaciBar)"; NRC grant 200672/S60. This paper is also a contribution to the Centre for Arctic Gas Hydrate, Environment and Climate (CAGE). Thanks to the University Centre in Svalbard and the Geological Survey of Norway for providing an office during part of the PhD work. We thank two anonymous reviewers, whose comments greatly improved the paper. Last but not least, thanks to our Russian collaborators during the 18th Training Through Research (TTR) cruise to the Barents Sea, to the captain and crew of the University of Tromsø R/V Helmer Hanssen and to engineer Steinar Iversen for help with data acquisition and processing.

References

Alley, R.B., Blankenship, D.D., Bentley, C.R., Rooney, S.T., 1986. Deformation of till beneath ice stream B, West Antarctica. Nature 322, 57-59.

Anandakrishnan, S., Alley, R.B., Jacobel, R.W., and Conway, H.,2001. The flow regime of Ice Stream C and hypotheses concerning its recent stagnation, *in* Alley, R.B., and Bindschadler, R.A., eds., The West Antarctic Ice Sheet: Behavior and environment: American Geophysical Union Antarctic Research Series, **77,** 283-294

Andersen, B. G., 1981. Late Weichselian Ice Sheets in Eurasia and Greenland. In: Denton, G. H., Hughes, T. J. (Eds.), The Last Great Ice Sheets. John Wiley and Sons, New York, pp. 1-65.

Andreassen, K., Ødegaard, C. M., Rafaelsen, B., 2007. Imprints of former ice streams, imaged and interpreted using industry three-dimensional seismic data from the south-western Barents Sea, *in*: Davies, R. J., Posamentier, H. W., Wood, L. J., and Cartwright, J. A. (eds), Seismic Geomorphology: Applications to Hydrocarbon Exploration and Production. Geological Society, London, Special Publications 277, 151-169.

Andreassen, K., Laberg, J.S., Vorren, T., 2008. Seafloor geomorphology of the SW Barents Sea and its glaci-dynamic implications. Geomorphology 97, 157-177.

Andreassen, K., Winsborrow, M.C.M., 2009. Signature of ice streaming in Bjørnøyrenna, Polar North Atlantic, through the Pleistocene and implications for ice-stream dynamics. Annals of Glaciology 50, 17-26.

Andreassen, K., Winsborrow, M.C.M., Bjarnadóttir, L.R., Rüther, D.C., This volume. Ice stream reatreat dynamics inferred from an assemblage of landforms in the northern Barents Sea, This volume.

Barnes, P.W., Lien, R., 1987. Icebergs rework shelf sediments to 500 m off Antarctica. Geology 16, 1130-1133.

Bell, R. E., 2008. The role of subglacial water in ice-sheet mass balance, Nature 1, 297-313.

Bennett, M. R., 2003. Ice streams as the arteries of an ice sheet: their mechanics, stability and significance. Earth-Science Reviews 61, 309-339.

Bindschadler, R., 2006. Climate change - Hitting the ice sheets where it hurts. Science 311, 1720-1721.

Bjarnadóttir, L.R. 2012, Processes and dynamics during deglaciation of a polar continental shelf. Examples from the marine-based Barents Sea Ice Sheet. Ph.D. Thesis, Geology Department, Faculty of Science and Technology, University of Tromsø, Norway, p. 144. ISBN: 978-82-8236-080-7.

Bjarnadóttir, L.R., Winsborrow, M.C.M., Andreassen, K., 2012. Tunnel valleys in the Barents Sea, In: Bjarnadóttir, L.R. 2012, Processes and dynamics during deglaciation of a polar continental shelf. Examples from the marine-based Barents Sea Ice Sheet. Ph.D. Thesis, Geology Department, Faculty of Science and Technology, University of Tromsø, Norway, p. 144. ISBN: 978-82-8236-080-7.

Bjarnadóttir, L.R., Rüther, D.C., Winsborrow, M.C.M., Andreassen, K., 2013. Grounding line dynamics during the last deglaciation of Kveithola, W Barents Sea, as revealed by seabed geomorphology and shallow seismic stratigraphy. Boreas 42 (1), 84-107.

Bondevik, S., Mangerud, J., Ronnert, L., Salvigsen, O., 1995. Postglacial sea-level history of Edgeøya and Barentsøya, eastern Svalbard. Polar Research 14, 153-180.

Bougamont, M., Tulaczyk, S., Joughin, I.,2003. Response of subglacial sediments to basal freeze-on 2. Application in numerical modeling of the recent stoppage of Ice Stream C, West Antarctica. Journal of geophysical research 108 No. B4, 2223, doi: 10.1029/2002JB001936.

Boulton, G.S., 1986. Push-moraines and glacier-contact fans in marine and terrestrial environments. Sedimentology 33, 667-698.

Bradwell, T., Stoker, M.S., Golledge, N.R., Wilson, C.K., Merritt, J.W., Long, D., Everest, J.D., Hestvik, O.B., Stevenson, A.G., Hubbard, A.L., Finlayson, A.G., Mathers, H.E., 2008. The northern sector of the last British Ice Sheet: Maximum extent and demise. Earth-Science Reviews 88, 207-226.

Clark, C.D., Tulaczyk, S., Stokes, C.R., Canals, M., 2003. A groove-ploughing theory for the production of mega-scale glacial lineations, and implications for ice-stream mechanics. Journal of Glaciology 49, 240-256.

Conway, H., and Rasmussen, L. A., 2009. Recent thinning and migration of the Western Divide, central West Antarctica. Geophysical Research Letters 36, L12502, doi: 10.1029/2009GL038072.

De Angelis, H., Skvarca, P., 2003. Glacier surge after ice shelf collapse. Science 299, 1560-1562.

Dowdeswell, J.A., Ottesen, D., Evans, J., Ó Cofaigh, C., Anderson, J.B., 2008. Submarine glacial landforms and rates of ice-stream collapse. Geology 36, 819-822.

Dowdeswell, J.A., Hogan, K.A., Evans, J., Noormets, R., Ó Cofaigh, C., Ottesen, D., 2010. Past ice-sheet flow east of Svalbard inferred from streamlined subglacial landforms. Geology 38, 163-166.

Dowdeswell, J. A. and Fugelli, E.M.G., 2012. The seismic architecture and geometry of grounding-zone wedges formed at the marine margins of past ice sheets. Geological Society of America Bulletin 124, 170-1761.

Elverhøi, A., Solheim, A., 1983. The Barents Sea ice sheet - a sedimentological discussion. Polar Research 1, 23-42.

Elverhøi, A., Fjeldskaar, W., Solheim, A., Nyland-Berg, M., Russwurm, L., 1993. The Barents Sea Ice Sheet - A model of its growth and decay during the Last Glacial Maximum. Quaternary Science Reviews 12, 863-873.

Epshtein, O.G., Dlucagh, A.G., Starovoytov, A.V., Romanyuk, B.F., 2011a. Pleistocene Sediments of the Eastern Barents Sea (Central Deep and Murmansk Bank Areas): Communication 1. Occurence Conditions and Main Structural Features. Lithology and Mineral Resources 46, 115-134.

Epshtein, O.G., Dlucagh, A.G., Starovoytov, A.V., Romanyuk, B.F., 2011b. Pleistocene Sediments of the Eastern Barents Sea (Central Deep and Murmansk Bank): Communication 2. Lithological Composition and Formation Conditions. Lithology and Mineral Resources 46, 220-249.

Fricker, H. A., Scambos, T., Bindschadler, R., Padman, L., 2007. An Active Subglacial Water System in West Antarctica Mapped from Space, Science 315, 1544-1548.

Forman, S.L., Lubinski, D.J., Miller, G.H., Snyder, J., Matishov, G., Korsun, S., Myslivets, V., 1995. Postglacial emergence and distribution of late Weichselian ice-sheet loads in the northern Barents and Kara seas, Russia. Geology 23, 113-116.

Geirsdóttir, Á., Miller, G.H., Wattrus, N.J., Björnsson, H., Thors, K., 2008. Stabilization of glaciers terminating in closed water bodies: Evidence and broader implications. Geophysical Research Letters 35.

Hogan, K.A., Dowdeswell, J.A., Noormets, R., Evans, J., Ó Cofaigh, C., 2010a. Evidence for full-glacial flow and retreat of the Late Weichselian Ice Sheet from the waters around Kong Karls Land, eastern Svalbard. Quaternary Science Reviews 29, 3563-3582.

Hogan, K.A., Dowdeswell, J.A., Noormets, R., Evans, J., Ó Cofaigh, C., Jakobsson, M., 2010b. Submarine landforms and ice-sheet flow in the Kvitøya Trough, northwestern Barents Sea. Quaternary Science Reviews 29, 3545-3562.

Hubbard, B.P., Sharp, M.J., Willis, I.C., Nielsen, M.K., Smart, C.C., 1995. Borehole water-level variations and the structure of the subglacial hydrological system of Haut Glacier d´Arolla, Valais, Switzerland. Journal of Glaciology 41, 572-583.

Hulbe, C., Fahnestock, M., 2007. Century-scale discharge stagnation and reactivation of the Ross ice streams, West Antarctica, Journal of geophysical research 112, F03S27, doi: 10.1029/2006JF000603.

Ingólfsson, Ó., Landvik, J. Y., 2013. The Svalbard-Barents Sea ice-sheet - Historical, current and future perspectives. Quaternary Science Reviews 64, 33-60.

Jakobsson, M., Anderson, J.B., Nitsche, F.O., Dowdeswell, J.A., Gyllencreutz, R., Kirchner, N., Mohammad, R., O´Regan, M., Alley, R.A., Anandakrishnan, S., Eriksson, B., Kirshner, A., Fernandez, R., Stolldorf, T., Minzoni, R., Majewski, W., 2011. Geological record of ice shelf break-up and grounding line retreat, Pine Island Bay, West Antarctica. Geology 39, 691-694.

Jakobsson, M., Mayer, L., Coakley, B., Dowdeswell, J.A., Forbes, S., Fridman, B., Hodnesdal, H., Noormets, R., Pedersen, R., Rebesco, M., Schenke, H.W., Zarayskaya, Y., Accettella, D., Armstrong, A., Anderson, R.M., Bienhoff, P., Camerlenghi, A., Church, I., Edwards, M., Gardner, J.V., Hall, J.K., Hell, B., Hestvik, O.B., Kristoffersen, Y., Marcussen, C., Mohammad, R., Mosher, D., Nghiem, S.V., Pedrosa, M.T., Travaglini, P.G., Weatherall, P., 2012. The International Bathymetric Chart of the Arctic Ocean (IBCAO) Version 3.0. Geophysical Research Letters 39, LI2609.

Joughin, I., Tulaczyk, S., 2002. Positive Mass Balance of the Ross Ice Streams, West Antarctica, Science 295, (no. 5554), 476-480. DOI: 10.1126/science.1066875.

Joughin, I., Tulaczyk, S., Bindschadler, R., Price, S. F., 2002. Changes in west Antarctic ice stream velocities: Observation and analysis, Journal of geophysical research 107, No. B11, 2289, doi: 10.1029/2001JB001029.

Kristoffersen, Y., Milliman, J.D., Ellis, J.P., 1984. Unconsolidated sediments and shallow structure of the northern Barents Sea. Norsk Polarinstitutt Skrifter 180, 25-39.

Lambeck, K., 1995. Constraints on the Late Weichselian ice sheet over the Barents Sea from observations of raised shorelines. Quaternary Science Reviews 14, 1-16.

Lambeck, K., 1996. Limits on the areal extent of the Barents Sea ice sheet in Late Weichselian time. Global and Planetary Change 12, 41- 51.

Landvik, J.Y., Bondevik, S., Elverhøi, A., Fjeldskaar, W., Mangerud, J., Salvigsen, O., Siegert, M.J., Svendsen, J.I., Vorren, T.O., 1998. The last glacial maximum of Svalbard and the Barents Sea area: Ice sheet extent and configuration. Quaternary Science Reviews 17, 43-75.

Livingstone, S.J., Ó Cofaigh, C., Stokes, C.R., Hillenbrand, C.-D., Vieli, A., Jamieson, S.S.R., 2012. Antarctic palaeo-ice streams. Earth-Science Reviews 111, (1-2), 90-128, doi:10.1016/j.earscirec.2011.10.003

Mangerud, J., Dokken, T., Hebbeln, D., Heggen, B., Ingólfsson, Ó.,Landvik, J. Y., Mejdahl, V., Svendsen, J. I., Vorren, T. O., 1998. Fluctuations of the Svalbard Barents Sea Ice Sheet during the last 150 000 years. Quaternary Science Reviews 17, 11-42.

Mangerud, J., Bondevik, S., Gulliksen, S., Hufthammer, A. K., Høiseter, T., 2006. Marine 14C reservoir ages for 19th century whales and molluscs from the North Atlantic. Quaternary Science Reviews 25, 3228-3245.

Mercer, J. H., 1970. A former ice sheet in the Arctic Ocean? Palaeogeography, Palaeoclimatology, Palaeoecology 8, 19-27.

O´Cofaigh, C., Pudsey, C.J., Dowdeswell, J.A., Morris, P., 2002. Evolution of subglacial bedforms along a paleo-ice stream, Antarctic Peninsula continental shelf. Geophysical Research Letters 29, art. no.-1199.

O´Cofaigh, C., Dowdeswell, J.A., Evans, J., Larter, R.D., 2008. Geological constraints on Antarctic palaeo-ice-stream retreat. Earth Surface Processes and Landforms 33, 513-525.

Ottesen, D., Dowdeswell, J.A., Rise, L., 2005. Submarine landforms and the reconstruction of fast-flowing ice streams within a large Quaternary ice sheet: The 2500-km-long Norwegian-Svalbard margin (57 degrees-80 degrees N). Geological Society of America Bulletin 117, 1033-1050.

Ottesen, D., Dowdeswell, J.A., 2006. Assemblages of submarine landforms produced by tidewater glaciers in Svalbard. Journal of Geophysical Research 111.

Ottesen, D., Dowdeswell, J.A., 2009. An inter-ice-stream glaciated margin: Submarine landforms and a geomorphic model based on marine-geophysical data from Svalbard. Geological Society of America Bulletin 121, 1647-1665.

Patterson, C.J., 1997. Southern Laurentide ice lobes were created by ice streams: Des Moines lobe in Minnesota, USA. Sedimentary Geology 111, 249-261.

Payne, A.J., Vieli, A., Shepherd, A.P., Wingham, D.J., Rignot, E., 2004. Recent dramatic thinning of largest West Antarctic ice stream triggered by oceans. Geophysical Research Letters 31, art. no.-L23401.

Piotrowski, J.A., Larsen, N.K., Junge, F.W., 2004. Reflections of soft subglacial beds as a mosaic of deforming and stable spots. Quaternary Science Reviews 23, 993-1000.

Polyak, L., Lehman, S. J., Gataullin, V., Timothy Jull, A. J., 1995. Two-step deglaciation of the southeastern Barents Sea. Geology 23 (6), 567-571.

Powell, R.D., Alley, R.A., 1997. Grounding-line systems: processes, glaciological inferences and the stratigraphic record. Geology and seismic stratigraphy of the Antarctic margin, Part 2. Antarctic Research Series 71, 169-187.

Reimer, P. J., Baillie, M. G. L., Bard, E. et al., 2009. IntCal09 and Marine09 radiocarbon age calibration curves, 0-50,000 years cal BP. Radiocarbon, 1111-1150.

Retzlaff, R., Bentley, C. R., 1993. Timing of stagnation of ice stream C, West Antarctica, from short-pulse radar studies of buried surface crevasses. Journal of Glaciology 39 (133), 553-561.

Rignot, E., Casassa, G., Gogineni, P., Krabill, W., Rivera, A., Thomas, R., 2004. Accelerated ice discharge from the Antarctic Peninsula following the collapse of Larsen B ice shelf. Geophysical Research Letters 31, art. no.-L18401.

Rüther, D.C., Mattingsdal, R., Andreassen, K., Forwick, M., Husum, K., 2011. Seismic architecture and sedimentology of a major grounding zone system deposited by the Bjørnøyrenna Ice Stream during Late Weichselian deglaciation. Quaternary Science Reviews 30, 2776-2792.

Rüther, D.C., 2012. Changing ice stream flow regimes during the last deglaciation of Bjørnøyrenna, western Barents Sea. In: Palaeoenvironment of the Barents Sea during the last deglaciation and Holocene. Processes and timing. PhD-thesis, Department of Geology, Faculty of Science and Technology. University of Tromsø, Tromsø, p. 116. ISBN: 978-82-8236-060-9.

Salvigsen, O., 1981. Radiocarbon dated raised beaches in Kong Karls Land, Svalbard, and their consequences for the glacial history of the Barents Sea area. Geografiska Annaler 63A (3-4), 283-291.

Salvigsen, O., Adrielsson, L., Hjort, C., Kelly, M., Landvik, J. Y., Ronnert, L. , 1995. Dynamics of the last glaciation in eastern Svalbard as inferred from glacier-movement indicators. Polar Research 14, 141-152.

Scambos, T., Hulbe, C., Fahnestock, M., 2003. Climate-induced ice shelf disintegration in the Antarctic peninsula. Antarctic research series 76, 335-347.

Scambos, T.A., Bohlander, J.A., Shuman, C.A., Skvarca, P., 2004. Glacier acceleration and thinning after ice shelf collapse in the Larsen B embayment, Antarctica. Geophysical Research Letters 31, art. no.-L18402.

Sharp, M., 1985. "Crevasse-fill" ridges - a landform type characteristic of surging glaciers? Geografiska Annaler 67A, 213-220.

Siegert, M. J., Dowdeswell, J. A., Svendsen, J.-I., Elverhøi, A., 2002. The Eurasian Arcic During the Last Ice Age: A vast ice sheet once covered the Barents Sea. Its sudden disappearance 100 centuries ago provides a lesson about western Antarctica today. American Scientist 90 (1), 32-39.

Sigmond, E.M.O., 2002. Geological Map, Land and Sea Areas of Northern Europe, Scale 1:4 million. Geological Survey of Norway.

Smith, A. M., Murray, T., Nicholls, K. W., Makinson, K., Aðalgeirsdóttir, G., Behar, A. E., Vaughan, D. G., 2007. Rapid erosion, drumlin formation, and changing hydrology beneath an Antarctic ice stream. Geology 35, 127-130.

Smith, B. E., Fricker, H. A., Joughin, I. R., Tulaczyk, S., 2009. An inventory of active subglacial lakes in Antarctica detected by ICESat (2003-2008). Journal of Glaciology 55 (192), 573-595.

Stearns, L. A., Smith, B. E., Hamilton, G. S., 2008. Increased flow speed on a large East Antartic outlet glacier caused by subglacial floods, Nature Geoscience 1, 827-831.

Solheim, A., Russwurm, L., Elverhøi, A., Berg, M.N., 1990. Glacial geomorphic features in the northern Barents Sea: direct evidence for grounded ice and implications for the pattern of deglaciation and late glacial sedimentation, In: Dowdeswell, J.A., Scourse, J.D. (Eds.), Glacimarine Enviroments: Processes and Sediments. The Geological Society, London.

Solheim, A., Kristoffersen, Y., 1984. Physical environment Western Barents Sea, 1:1,500,000; Sediments above the upper regional unconformity: thickness, seismic stratigraphy and outline of the glacial history. Norsk Polarinstitutt Skrifter 179B, 3-26.

Solheim, A., Pfirman, S.L., 1985. Sea-floor morphology outside a grounded, surging glacier, Bråsvellbreen, Svalbard. Marine Geology 65, 127-143.

Stokes, C.R., Clark, C.D., 1999. Geomorphological criteria for identifying Pleistocene ice streams. Annals of Glaciology 28, 67-74.

Stokes, C.R., Clark, C.D., 2001. Palaeo-ice streams. Quaternary Science Reviews 20, 1437-1457.

Stuiver, M. and Reimer, P. J., 1993. Extended 14C database and revised CALIB radiocarbon calibration program. Radiocarbon 35, 215-230.

Svendsen, J.I., Gataullin, V., Mangerud, J., Polyak, L., 2004. The glacial History of the Barents and Kara Sea Region, In: Ehlers, J., Gibbard, P.L. (Eds.), Developments in Quaternary Sciences. Elsevier, pp. 369-378.

Van der Veen, C.J., 1998. Fracture mechanic approach to penetration of bottom crevasses on glaciers. Cold Regions Science and Technology 27, 213-223.

Vorren, T. O., Hald, M., Lebesbye, E., 1988. Late Cenozoic environments in the Barents Sea. Paleoceanography 3, 601-612.

Vorren, T. O., Laberg, J. S., 1996. The Middle and Late Pleistocene evolution of the Bear Island Trough Mouth Fan. Global and planetary Change 12, 309-330.

Wellner, J.S., Heroy, D.C., Anderson, J.B., 2006. The death mask of the antarctic ice sheet: Comparison of glacial geomorphic features across the continental shelf. Geomorphology 75, 157-171.

Winsborrow, M.C.M., Andreassen, K., Corner, G.D., Laberg, J.S., 2010. Deglaciation of a marine-based ice sheet: Late Weichselian palaeo-ice dynamics and retreat in the southern Barents Sea reconstructed from onshore and offshore glacial geomorphology. Quaternary Science Reviews 29, 424-442.

Olex: A bathymetry database of echo-soundings, 2012. Made and managed by Olex AS, Trondheim, Norway, http://www.olex.no.

Figure captions

Fig. 1. Map of study areas in the central Barents Sea. Areas 1-5 (Figs. 2-8) are indicated with black polygons. The white broken line represents the ice extent during the Last Glacial Maximum (LGM; Svendsen et al., 2004). Also shown are the old border of the disputed area and new territorial border between Norway and Russia.

Fig. 2. Area 1 - seafloor geomorphology. a) Geomorphic map of area 1, the location of which is indicated in red on the miniature polygon map of areas 1-5. Interpreted ice margin positions are shown with white numbers (1-8). Ice margin positions 2-5 and 9 are modified from Rüther (2012) and Andreassen et al. (This volume), respectively. Black rectangle shows location of b-g. b) Corrugation ridges, ice-fingerprints and recessional ridges; c) Linear stagnation ridges; d) Needle (indicated by black arrow) and a transverse profile across the needle is shown; e) Corrugated, uniform furrows, profile shows a number of corrugation ridges; f) Polygonal stagnation ridge

network; g) Uniform ploughmarks downstream of an ATB. Artifacts due to erroneous swath-edge soundings are indicated by black arrows with baselines.

Fig. 3. Area 1- sediment characteristics. a) Distribution of acoustically transparent sediment bodies (ATBs) based on chirp data and single-channel seismic data. The location of area 1 is indicated by a red fill on a miniature polygon map of areas 1-5. Ice margin positions 2-5 and 9 were modified from Rüther (2012) and Andreassen et al. (This volume), respectively. b-f) Chirp transect across selected ATBs.

Fig. 4. Area 2. a) Geomorphic map of area 2, location indicated by a red fill on the miniature polygon map of areas 1-5. The location of chirp/seismic profiles shown in c, and e-g, and location of close-ups b and d are indicated; b) Multibeam swath bathymetry data showing streamlining by ice-fingerprints (arrowed). The white dotted line shows the location of chirp profile c; c) Chirp profile across several ice-fingerprints (arrowed); d) Multibeam swath bathymetry data showing examples of wide ice-fingerprints (arrowed). The white dotted line shows the location of profile e; e) Chirp profile across several ice-fingerprints (arrowed); f) Chirp profile showing the ATB and innermost retreat moraine; g) Seismic line from SW-NE across Storbankrenna. Note the large bedrock ridges covered with thin sediments and thicker ATB in the eastern part (arrowed). Black rectangle shows the location of profile g.

Fig. 5. Area 3. a) Geomorphic map of area 3, location indicated by a red fill on the miniature polygon map of areas 1-5. b) Mapped recessional ridges. Dotted rectangle shows the location of fig 5c; c) Multibeam swath bathymetry data showing several successive curvilinear recessional moraines (red arrows) and ice-fingerprints (black arrows). Black line shows the location of profile d; d) Chirp profile across recessional ridges and ice-fingerprints, red and black arrows point to the same recessional ridges/ice-fingerprints arrowed in Fig. 5c.

Fig. 6. Area 4. a) Geomorphic map of area 4,location indicated by a red fill on the miniature polygon map of areas 1-5. The location of seismic/chirp lines in Fig. 7 are indicated (red lines). Dotted black rectangles indicate locations of Fig. 6b, c and d; b) Close-up showing distribution of MSGLs, number of GZWs and simplified ploughmarks directions; c) Multibeam swath bathymetry data showing MSGLs; d) Multibeam swath bathymetry data showing example of uniform ploughmarks.

Fig. 7. Seismic data in area 4. a-e) Single channel seismic and chirp lines. Yellow dotted line indicates upper boundary of bedrock. In a) a white line indicates boundary between GZW3 and GZW4. Black dotted rectangle shows extent of profile 7b, the location of MSGLs shown in Fig. 6b is indicated. In b) red arrows point to boundaries between GZWs.

Fig. 8. Area 5. a) Geomorphic map of area 5, location indicated by a red fill on the miniature polygon map of areas 1-5; b-e) Red lines show location of seismic lines from the TTR-18 cruise. Arrows point to ATBs, yellow dotted lines mark ATB lower boundaries.

Fig. 9. Reconstructed pattern of deglaciation showing main palaeo-ice flow directions and dynamics. Palaeo-glacial dynamics are indicated by shaded polygons where areas where ice flow was either 1) fast and dynamic (medium grey), sometimes with stagnation (dark-grey), or 2) slow with formation of retreat ridges (light grey).

Fig. 10. Simplified conceptual model of ice stream velocity cycles The model is based on Bjørnøyrenna Ice Stream during the late stages of deglaciation. The circle describes a full cycle with main states of ice flow velocity (uppercase letters) and the consequence of such a state (lowercase letters). The grey stippled rectangle denotes the part of the cycle where an ice shelf forms by lift-off of stagnant ice, and its consequent disintegration. There are many possible feedbacks and loops

within this cycle, as indicated by the arrows within the circle, meaning that ice streams did not necessarily always go through all states in each cycle.

*Figure1
Click here to download high resolution image

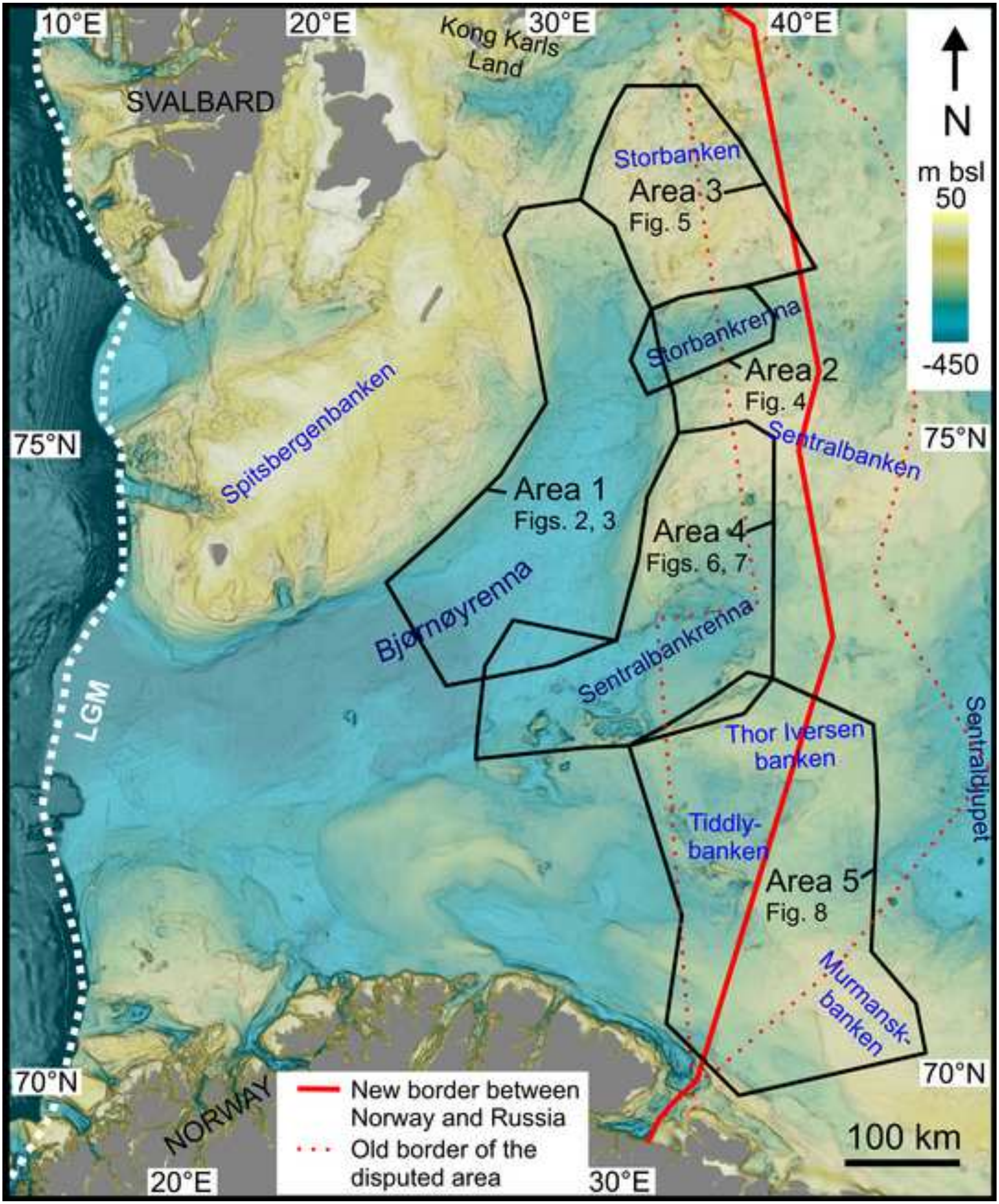

*Figure2
Click here to download high resolution image

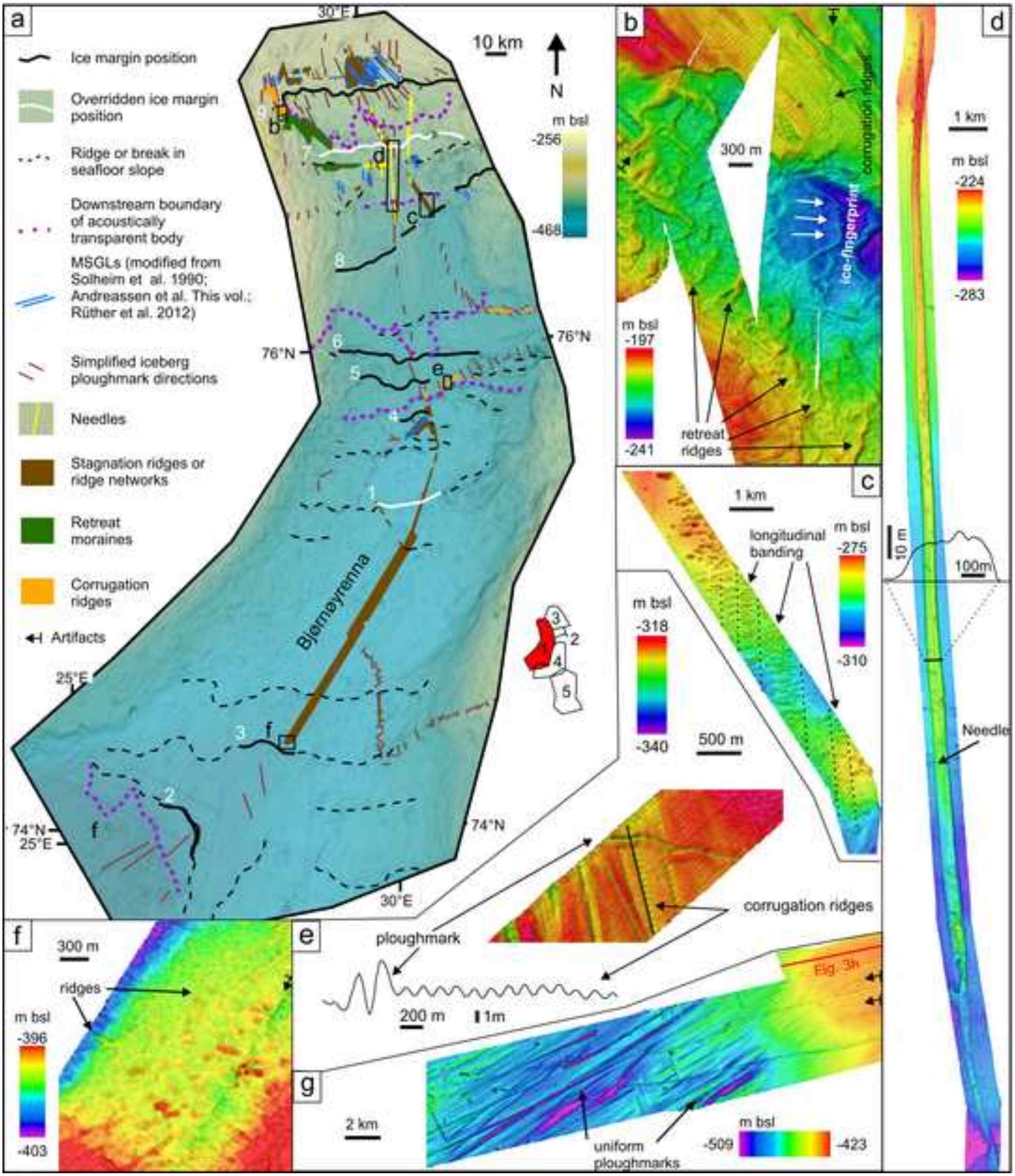

*Figure3
Click here to download high resolution image

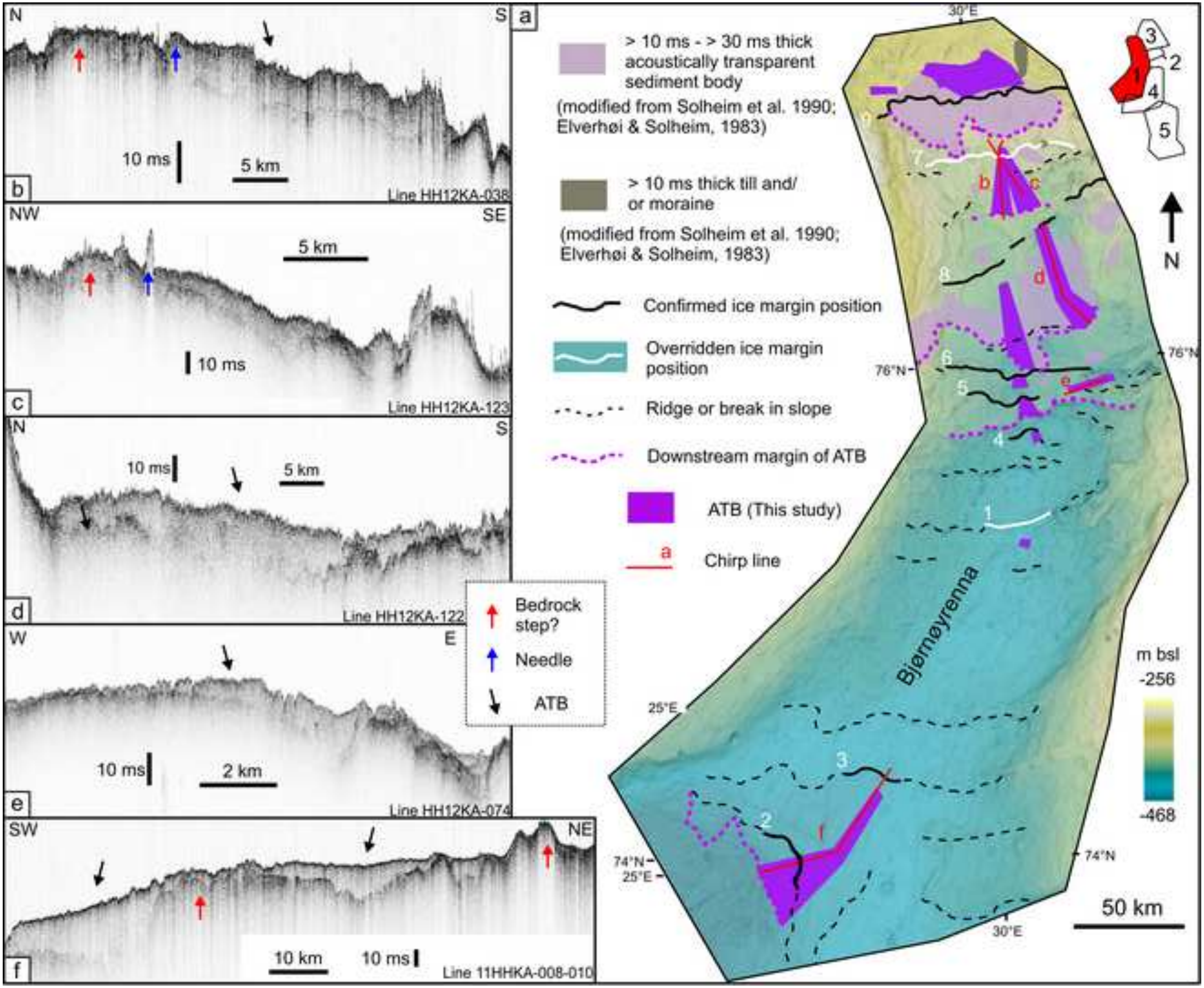

***Figure4**

Click here to download high resolution image

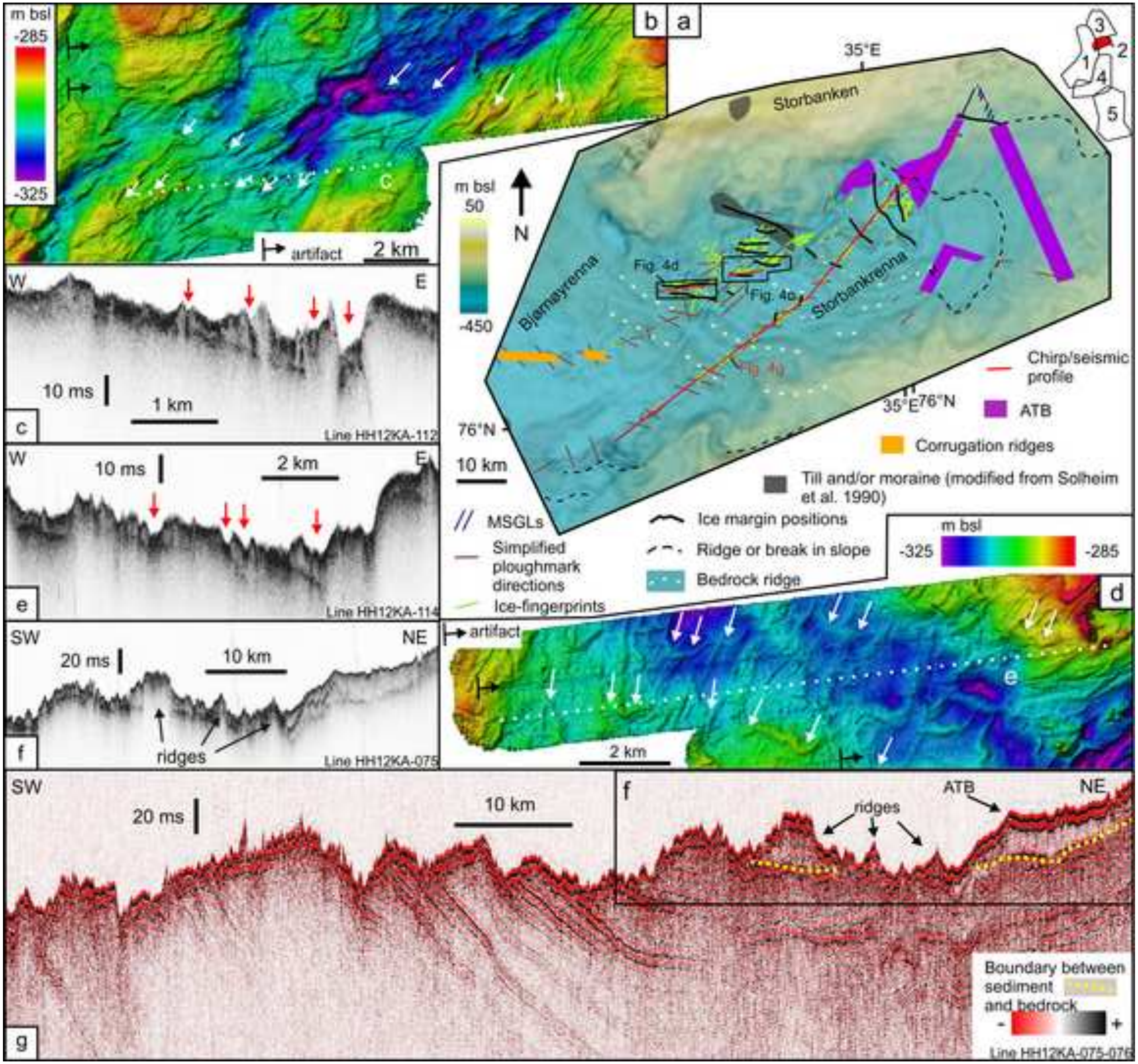

*Figure5

Click here to download high resolution image

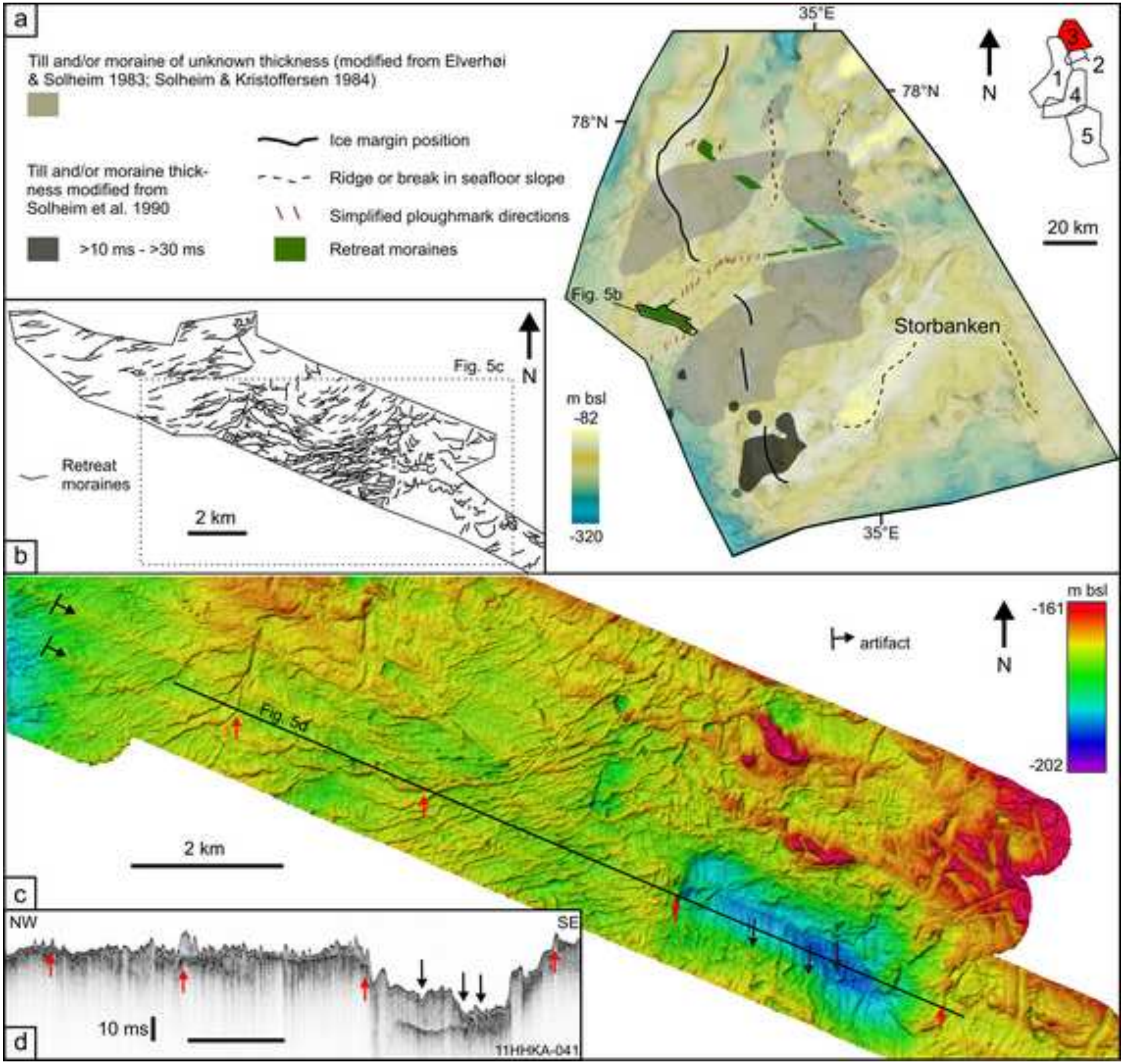

*Figure6

Click here to download high resolution image

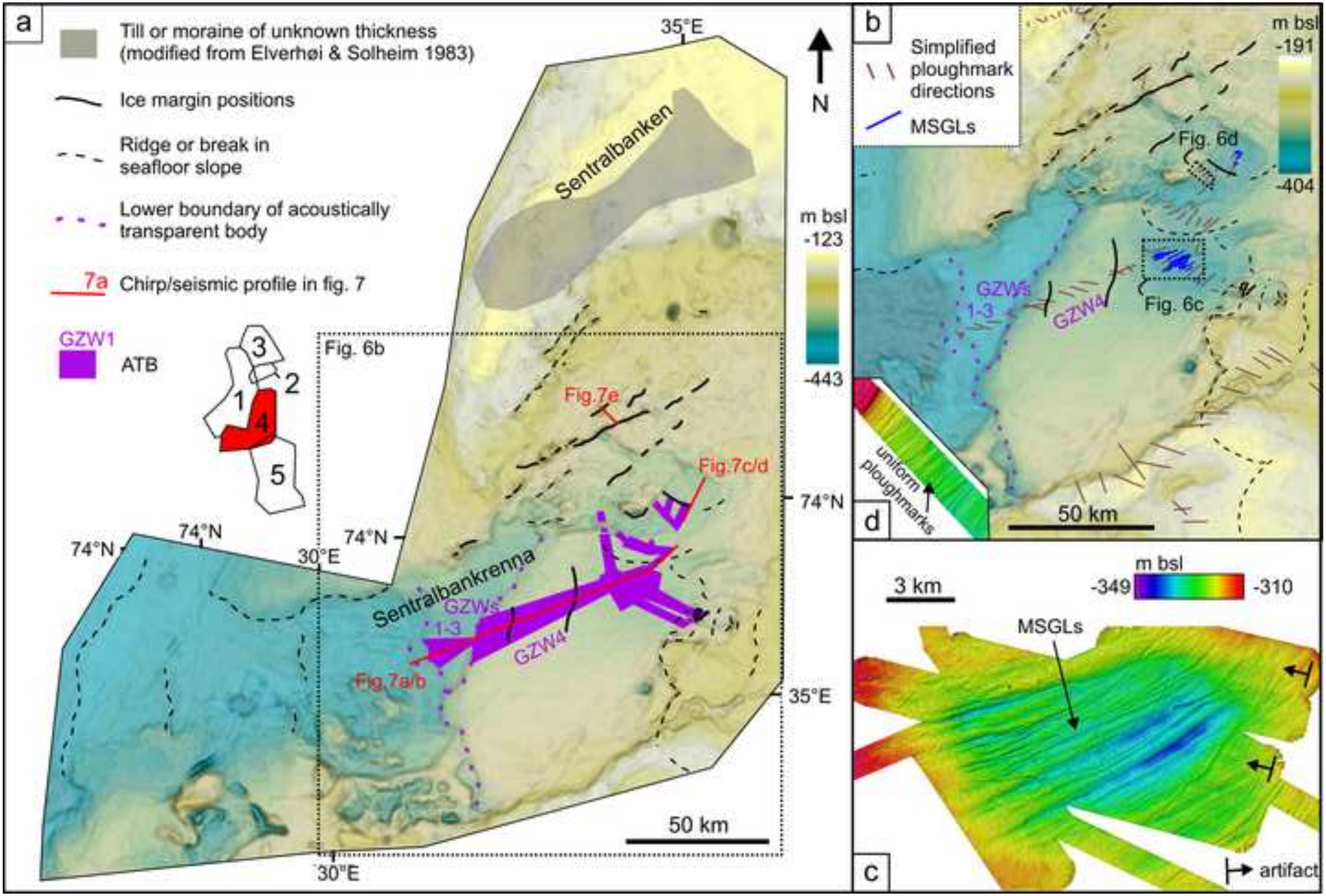

***Figure7**

Click here to download high resolution image

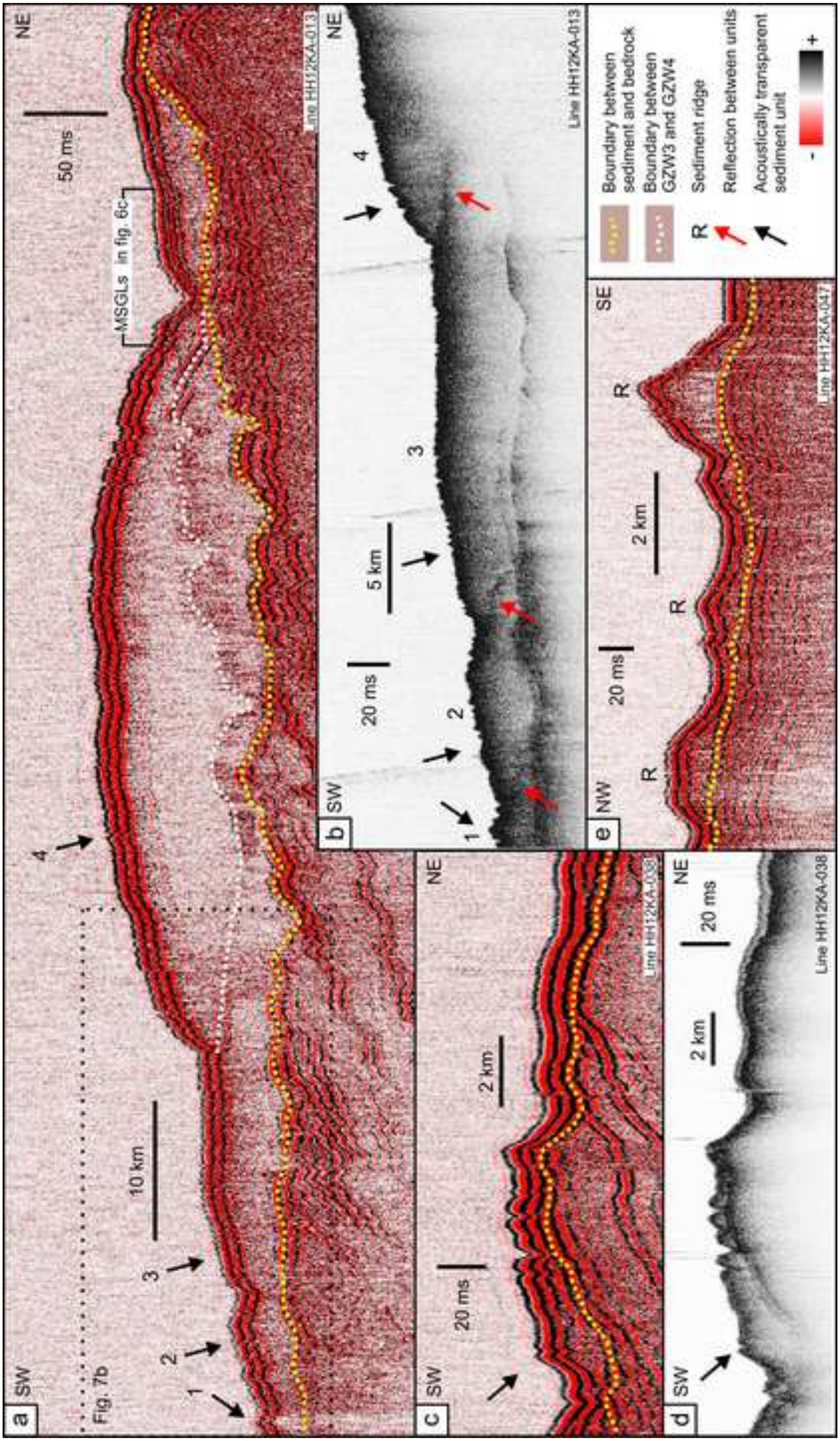

*Figure8
Click here to download high resolution image

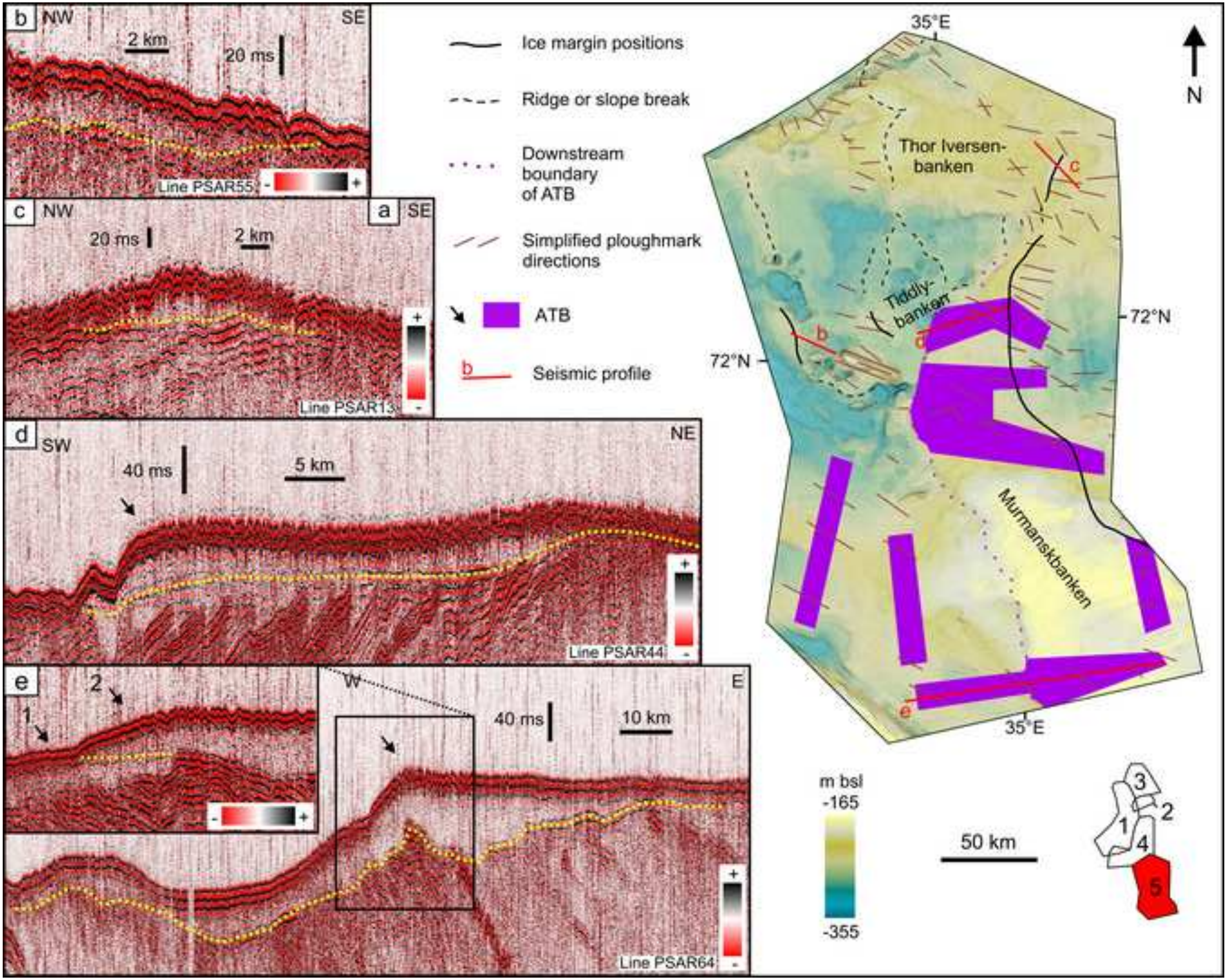

*Figure9
Click here to download high resolution image

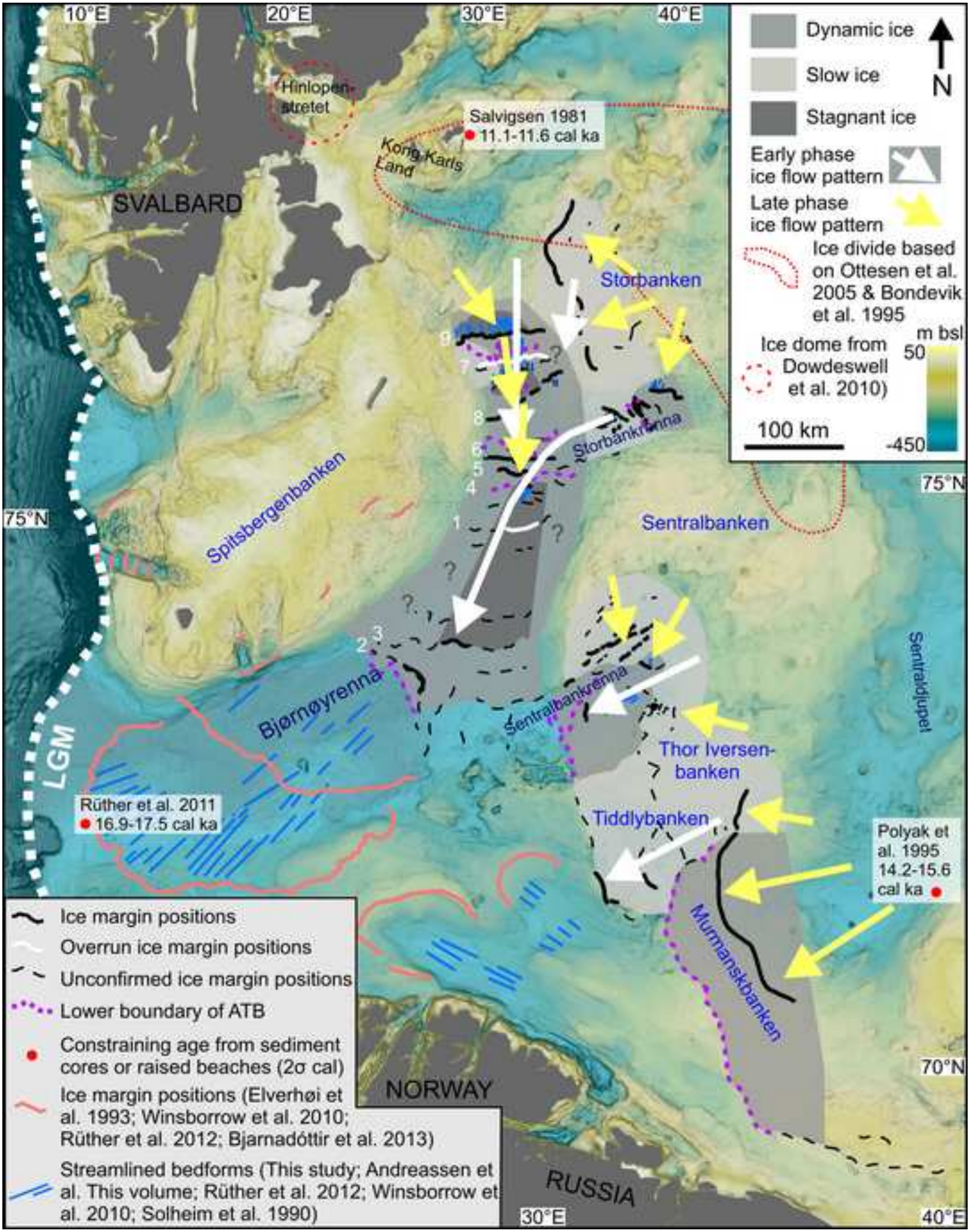

*Figure10
Click here to download high resolution image